PERFORMANCE STUDY OF A WIND-DIESEL HYBRID POWER SYSTEM

A DISSERTATION

Submitted in partial fulfillment of the requirements for the award of the degree of

MASTER OF TECHNOLOGY

in

ELECTRICAL ENGINEERING

(With Specialization in Power System Engineering)

By

PURNACHANDER RAO.R

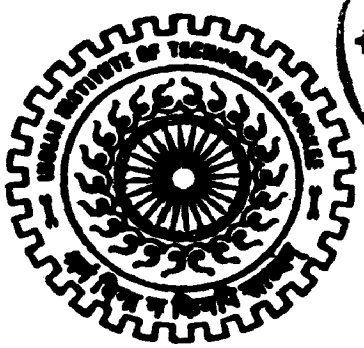

DEPARTMENT OF ELECTRICAL ENGINEERING
INDIAN INSTITUTE OF TECHNOLOGY ROORKEE
ROORKEE-247 667 (INDIA)

JUNE, 2006

ACKNOWLEDGEMENT

My foremost and profound gratitude goes to my guide **Dr. R. N. Patel,** Lecturer, Electrical Engineering Department, Indian Institute of Technology Roorkee, Roorkee, for his proficient and enthusiastic guidance, useful criticism, encouragement and immense help. I have deep sense of admiration for his innate goodness and inexhaustible enthusiasm. The valuable hours of discussions and suggestions that I had with him have undoubtedly helped in supplementing my thoughts in the right direction for attaining the desired objective. Working under his guidance will always remain a cherished experience in my memory and I will adore it throughout my life.

I express my deep sense of gratitude to the power system engineering group head Dr. J. D Sharma, Professor, Department of Electrical Engineering and Indian Institute of Technology, Roorkee, for his kind help in extending all the facilities possible to us. My heartfelt gratitude and indebtedness goes to all the teachers of **PSE** group who, with their encouraging and caring words, constructive criticism and suggestions, have contributed directly or indirectly in a significant way towards completion of this report.

Special, sincere and heartfelt gratitude goes to my parents, and my friends whose sincere prayers, best wishes, support and encouragement have been a constant source of assurance, guidance, strength, inspiration and upliftment to me.

I also thank all those who helped me directly or indirectly in the successful completion of my work.

R. P. C. Rao.

(Purnachander Rao.R)

Abstract

Hybrid sources of energies are rapidly increasing in power generating systems due to their viable option and wide spread public support for renewable energy. The goal of this thesis is to evaluate wind-diesel energy system through computer simulation studies. The primary focus of this study is the development of dynamic models for a standalone wind energy conversion system and a diesel generation system. The developed model of the wind energy conversion system consists of dynamic models for a wind turbine as well as an electric generator. A detailed model of the wind turbine is presented. The electric generator, driven by the wind turbine, is a line-excited induction generator suitable for hybrid system and grid-connected operations. A dynamic model for the diesel generation system is achieved by integrating models of a diesel engine and synchronous generator driven by it.

A set of mathematical equations are used to model a synchronous machine acting as the electric generator for the diesel generation system. The developed system is capable of simulating the dynamics of the wind-diesel generation system, demonstrating its ability to meet load power requirements. The dynamic models of the wind energy conversion system and the diesel generation system are simulated in simulation tool called visual simulation (VisSim 6.0). In all electrical simulations d-q axis convention has been followed with the reference frame as synchronous reference frame. Simulation results indicate the suitability of the developed model to study the dynamic behavior of the hybrid generation system under different load conditions.

Contents

NOMENCLATURE

Cpf1	Power factor correcting capacitor
Vs_ref	Voltage set point
f_b	Frequency set point.
i_qsd	q component of current provided by synchronous generator/diesel module
i_dsd	d component of current provided by synchronous generator/diesel module
i_qs	q component of Transmission line current.
i_ds	d component of Transmission line current.
i_qv	q component of load current.
i_dv	d component of load current.
PCC	Point of common coupling
V_qs1	q component of voltage at the PCC module
Vs	System voltage
PFC1_KVAR	Reactive power generated by the PFC capacitor
SD_kW	Real power supplied by the diesel/synchronous generator
SD_kVAR	Reactive power provided by the diesel/synchronous generator
Pdiesel_rated	Power rating of diesel engine
$Gen_{m\_rad/sec}$	Angular velocity of diesel engine
T_{diesel}	Torque generated by the diesel engine
Synchronous Machine	
Eq_D	q component of generated voltage
Ke_D	Voltage flux constant
Lf	Field winding inductance
Rf	Field winding resistance
L_qSD	q component of stator inductance
L_dSD	d component of stator inductance
R_SD	Stator resistance

J_SD	Synchronous generator moment of inertia
Pole_SD	Poles of Synchronous generator
B_SD	Viscous friction coefficient of the synchronous generator
V_f	Field voltage of synchronous generator
V_wind	Wind speed
IG_kW	Real power provided by induction machine
IG_kVAR	Reactive power provided by induction machine
T_wind	High-velocity torque at the output of the gear box
Gear_r	Gear ratio
TSR	Tip speed ratio
Wr	Rotor speed of wind turbine
C_p	Performance co-efficient or aero dynamic efficiency
R_bld	Radius of the wind blade
ρ	Density of air
Induction Machine	
q	Quadrature axis
d	Direct axis
Ψ_{ds}	d component of stator flux linkages
Ψ_{qs}	q component of stator flux linkages
Ψ'_{dr}	q component of rotor flux linkages
Ψ'_{qr}	d component of rotor flux linkages
Ψ_{mq}	q component of Mutual flux linkages between stator and rotor
Ψ_{md}	d component of Mutual flux linkages between stator and rotor
i_{qi}	q component of stator current
i_{di}	d component of stator current
i'_{qr}	q component of rotor current

i'_{dr}	d component of rotor current
rs	Stator resistance
r'r	Rotor resistance
prime(')	prime indicates rotor components are referred to stator side
J	Rotor inertia
P	Number of Poles
Xm	Magnetizing reactance at base frequency
X'lr	Rotor leakage reactance at base frequency
X'lr	Stator leakage reactance at base frequency
V_ds2	d component of voltage at the Induction machine
V_qs2	q component of voltage at the Induction machine
P_{IG}	Real power of induction machine
Q_{IG}	Reactive power of induction machine
S_{IG}	Apparent power of induction machine
C_{pf2}	PFC capacitor at the wind turbine site
R_{LN}	Transmission line resistance
L_{LN}	Transmission line inductance.

LIST OF FIGURES

Chapter 01
Introduction

1.1 General

The ever increasing energy demands, dwindling sources of fossil fuels and concern about pollution levels in the environment has been the driving force behind electricity generation using renewable energy sources. Tapping the energy available from the renewable resources allows the attainment of notable reductions in the pollution levels and worrying climate changes. On the other hand, the availability of energy from renewable sources like wind energy, solar energy, etc. is unpredictable and is affected by factors beyond human control. Therefore, such renewable energy systems should be backed up by conventional sources of energy or energy storage devices in order to ensure continuity of the energy supply. This leads us to the topic of hybrid generation units comprising conventional or unconventional sources of energy or both, where two or more individual generation systems operate in parallel supplementing each other.

Especially the electricity generated from the diesel sets is more suitable for the places which are far away from grids and not economical to erect transmission lines. Such systems are often characterized by poor efficiency, high emissions and high maintenance costs because of prolonged operation at low load levels. In many such locations, the potential for renewable energy is high. Thus, this offers great incentives to reduce dependence on conventional fuels and to lower emissions. Hybrid power systems have been used very successfully to reduce pollution and to conserve diesel fuel consumption. In areas with good wind resources, wind energy can be an attractive addition to the existing diesel generator system. In remote and isolated areas far from the grid, it may not be an economically viable option to supply electric power from the grid. This is due to the high cost of transmission lines and higher transmission losses that accompany distribution of centrally generated power to remote areas. DGs come in different forms such as diesel fired turbines or on-site gas, reciprocating engines, microturbines, small hydro induction generators, wind turbines and fuel cells. Proper modeling of these DGs, which constitute hybrid generation systems, is needed in order to study their operation and impact on power systems.

Hybrid generation systems usually combine renewable sources like wind power with conventional sources of energy like diesel generation or gas turbines (or microturbines) to from an equivalent of a miniature (or virtual) grid. Such a configuration addresses two important issues namely, higher emissions because of conventional generation techniques and high cost of energy capture from renewable sources. For wind energy systems, the renewable source of energy considered in this thesis, the emissions are nil but it has relatively high capital costs. Diesel generation is the other generating system in the hybrid generation system. In this thesis, these two systems models are integrated to form a model of the hybrid generation system.

1.2 Literature review

Driesen *et al.,* [1] have made the observation that there is a renewed interest in small-scale electricity generation. The authors start with a survey of existing small-scale generation technologies and then move on with a discussion of the major benefits and issues of small-scale electricity generation. Different technologies are evaluated in terms of their possible contribution to the listed benefits and issues.

Patel *et al.,* [2] have analyzed the advantages and techno-economic constraints associated with the distributed generation. The distributed generator is given attention against a large-scale generator to correspond to uncertain demand growth. Distributed generation (DG), by way of setting up small generating units based on a variety of local energy sources with localized distribution, has been identified as the future shape of the power sector reforms and also as one of the alternatives for ensuring supply of power in rural areas.

Barker and Robert [3], have described a few of the issues that must be considered to insure that DG will not degrade distribution system power quality, safety or reliability. The authors focused on radial systems, although some of the issues discussed are common to low voltage distribution networks, and mainly on network voltage changes and harmonics.

Jenkins and Strbac [4] considered the impact of embedded generation on the power quality of distribution networks. The various types of embedded generation are discussed and their impact on the network reviewed. The potential for improvement of network power quality using embedded generators is addressed and the barriers to implementation briefly considered.

The web links [5]-[6] for the software and user manual guide for the VisSim Software is given in the references section. We can get the software from those links. VisSim is a visual block diagram language for modeling and simulation of complex nonlinear dynamic systems.

C. P. Butterfield *et al.*, [7] presented the operation of variable-speed wind turbines with pitch control. The system they had considered is controlled to generate maximum energy while minimizing loads. In low to medium wind speeds, the generator and the power converter control the wind turbine to capture maximum energy from the wind. In the high-wind-speed regions, the wind turbine is controlled to maintain the aerodynamic power produced by the wind turbine. Two methods to adjust the aerodynamic power were investigated: pitch control and generator load control, both of which are employed to regulate the operation of the wind turbine.

E.Muljadi *et al.,* [8] have analyzed a power system network consisted of wind and diesel power generation. Power quality and the interaction of diesel generation, the wind turbine, and the local load were the subjects of their investigation.

Slootweg *et al.* [9] presented a general model that can be used to represent all types of variable speed wind turbines in power system dynamic simulations. The wind turbine dynamics are approximated using nonlinear curves, which are numerical approximations, to estimate the value of wind turbine rotor efficiency for given values of rotor tip speed and pitch angle of the blade. The authors offer a comparison between the per-unit power curves of two commercial wind turbines and the one obtained theoretically by using the numerical approximation. The results indicate that a general numerical approximation can be used to simulate different types of wind turbines.

Tomas Petru and Thiringer [10] have presented the modeling of wind turbine for power system studies. And they have analyzed complexities of various parts of wind turbine model, such as aerodynamic conversion, drive train, and generator representation, are analyzed in their work. The results are verified by field measurements made on stall-regulated fixed speed wind turbine. And they have proved that their model is suitable for the use in grid simulation programs.

N. A. Schinas, N. A. Vovos, and G. B. Giannakopoulos [11] presented a control strategy for a variable speed pitch-controlled wind turbine (WT) generation scheme for the supply of an autonomous system with no energy storage units. In their

work they have used the synchronous generator which includes two three-phase stator windings displaced by 30^0 that are connected to the transformer load through two dc links with voltage source inverters (VSI). The first goal of the WT control system is to supply the load with constant real power under constant voltage as the wind speed varies between two levels and the second is to operate smoothly interchanging the load steps when the wind speed breaks through a speed level.

Kim Johnsen and Bo Eliasson [12] presented an aggregate wind farm model for use in real-time power system studies. The model they have developed in MATLAB/Simulink to operate with the ARISTO (advanced real-time interactive simulator for training and operation) simulator system. The wind farm model they have presented was based on the aggregate wind farm principle, on basis of the so-called "Danish concept" for wind turbines. Finally they discussed about their model with its performance.

Antonios E. *et al.,* [13] presents a model of the variable speed wind turbine connected to a permanent magnet synchronous generator (PMSG). But PMSGs suffer from uncontrollable magnetic field decaying over a period of time, their generated voltage tends to fall steeply with load and is not ideal for isolated operation. Induction generators, on the other hand, have many advantages over conventional synchronous generators due to their ruggedness, no need for DC filed current, low maintenance requirements and low cost.

P. C. Krause *et al.,* [14] demonstrated the effectiveness of an analog computer in studying the performance of induction machinery with computer simulation results which show the dynamic behavior of 2-phase and 3-phase machines during balanced and unbalanced operation. The computer simulation for these various modes of operation is conveniently obtained from the equations which describe the symmetrical induction machine in an arbitrary reference frame, and the simulations would be useful in studying the performance of induction machine when used in conjunction with electronic switching devices.

Anca D. Hansen *et al.,* [15] give a model of the WECS using doubly fed induction generator (DFIG). DFIGs allow one to produce power both from the stator and the rotor of a (wound rotor) induction generator. However increase in the power output comes with increased cost of power electronics, and their control, for the rotor circuit. One advantage of this configuration is its suitability for grid-connected operations where reactive power is supplied by the grid.

R.C.Bansal *et al.,* [16] have presented complete bibliography on the application of induction generators in non conventional energy systems. In this one they have given the bibliography of induction generators for wind power system applications and for hybrid power systems.

P. Kundur [17] describes the development of detailed mathematical model of synchronous machine and briefly reviews its steady state and transient performance characteristics. It defines the derived parameters of synchronous machine that are directly related to observed behavior under suitable test conditions and develops their relationships to the fundamental parameters. The simplifications required for the representation of the synchronous machine in stability studies are also discussed. It describes the characteristics and modeling of different types of synchronous generator excitation system as recommended by IEEE.

The generator model is derived starting from the basic circuit equations and the use of Park's transformation by K. R. Padiyar [18]. The models of excitation system and turbine governor system, the analysis of single machine connected to Infinite Bus and the study of transient stability by simulation are also presented in this book.

The book titled "Power System Control and Stability" [19] by P. M. Anderson and A. A. Fouad, a mathematical model for a synchronous machine is developed for stability studies. Two models are developed, one using the current as state variables and another using the flux linkages. Simplifies model, which are often used for stability studies are also discussed. It also covers some practical consideration in the use of the mathematical model of synchronous machines in stability studies.

H.E.McKenna *et al.,* [20] analyzed a power system network that consisted of two types of power generation: wind turbine generation and diesel generation. The power quality and the interaction of diesel generation, the wind turbine, and the local load were the subjects of their investigation. The purpose of their work is to show the impact of the wind power plant on the entire system. In addition, they discussed how the startup of the wind turbine and the transient condition during load changes affect the system's voltage and frequency.

Bialasiewic *et al.*, [21] presented a modular simulation system developed to study the dynamics and to aid in the design of hybrid power systems with diesel and wind turbine generation. The emphasis is placed on the representation of the dynamics of the elements of a real system and on the control aspects of the modules.

Various system configurations simulated in their work. And they have proved that, this tool can be used to study the transient and the steady-state interaction of the various components of a hybrid system.

Reference [22] presents a hybrid configuration comprising of a wind–diesel system originally developed by the Hydro-Quebec, aimed at reducing the cost of electricity supply in remote areas. The two main blocks of the system presented are, diesel- driven synchronous generator and the wind turbine driven by the asynchronous (induction) generator. The wind turbine block uses a 2-dimensional lookup table to compute the turbine torque output as a function of wind speed and turbine speed. In this all-wind mode, the synchronous machine is used as a synchronous condenser and its excitation system controls the grid voltage at its nominal value. A secondary load bank is used to regulate the system frequency by absorbing the wind power exceeding consumer demand.

C. Wang *et al.*, [23] investigated a small isolated hybrid power system that used a parallel combination of dispatchable and nondispatchable power generation sources. The interaction among different generation sources and the loads was investigated in their work. Simulation results showed the effect of the proposed system on voltage and frequency fluctuations.

A. Tomilson *et al.*, [24] developed a nonlinear dynamic model of the experimental wind-diesel system at the Atlantic Wind Test Site (AWTS) and simulated using the MATLAB and Simulink software packages. The model is validated by comparing the simulation with actual response measurements of the AWTS system.

G. S. Stavrakakis *et al.*, [25] presented detailed dynamic equations for the power system and Wind Energy Conversion System (WECS) components and their synthesis to a unified model are presented. This model is the basis for creating simulation software able to perform transient stability analysis of isolated Diesel-wind turbines power systems for accurate assessment of their interaction. A new general multimachine power system model is also developed which describes the topology and the complexity of Wind-Diesel systems in a compact form easy to implement in the simulation software.

1.3 Simulation tool

The simulation tool used in this work is the VisSim 6.0. Which is very powerful in implementing of mathematical equations, Vissim is a Windows-based program for modeling and simulating complex dynamic systems. Vissim combines an intuitive drag-and-drop block diagram interface with a powerful simulation engine. The visual interface offers a simple method for constructing, modifying and maintaining complex system models. The simulation engine provides fast and accurate solutions for linear, non-linear, continuous time, time varying and hybrid system design. [5] & [6]

With VisSim we can rapidly develop software prototypes of systems or processes to demonstrate their behavior prior to building the physical prototype. Further more, all modeling and simulation tasks can be completed without writing a line of code. This leads to significant savings in both development time and costs, and a greater assurance that the resultant product will perform as specified.

1.4 Organization of the Thesis

Chapter 1 describes the general introduction to the hybrid systems and its present importance to the power system. In this chapter we have also given the brief introduction to the new simulation software used for this work and last is the literature part.

Chapter 2 gives the definitions of distributed generation, hybrid systems, it's positive and negative impacts and also discusses the types of hybrid systems.

Chapter 3 is the heart of this report. It includes the modelling of all the components which are used in this work have been included with the mathematical equations and its corresponding simulation blocks.

Chapter 4 includes the case studies, results and discussion about results

Chapter 5 gives the conclusion of work considered and the future scope of work.

Chapter 2
HYBRID POWER SYSTEM

2.1 Distributed Generation

Distributed power generation is any small-scale power generation technology that provides electric power at a site closer to customers than central station generation. A distributed power unit can be connected directly to the consumer or to a utility's transmission or distribution system. One can further categorize distributed generation technologies as renewable and nonrenewable [1]-[2]. The distributed generation has positive impacts are generally called "system support benefits", and some of them are Loss reduction, Improved utility system reliability, Voltage support and improved power quality, Transmission and distribution capacity release, and Deferments of new or upgraded T&D infrastructure. Like the positive impacts DGs have negative impacts also and those include Generally results in higher energy costs, Less load diversity requires increased peak capacity, Requires redundancy for equivalent reliability, May require a utility connection for backup power, and May require a utility connection for load following.[3]-[4]

2.2 Renewable Technologies [2]

2.2.1 Wind Power

The terms "wind energy" or "wind power" describe the process by which the wind is used to generate mechanical power or electricity. Wind turbines convert the kinetic energy in the wind into mechanical power. This mechanical power can be used for specific tasks (such as grinding grain or pumping water) or a generator can convert this mechanical power into electricity to power homes.

Modern wind turbines fall into two basic groups; the horizontal-axis variety, like the traditional farm windmills used for pumping water, and the vertical-axis design, like the egg beater-style Darrieus model, named after its French inventor. Most large modern wind turbines are horizontal-axis turbines.

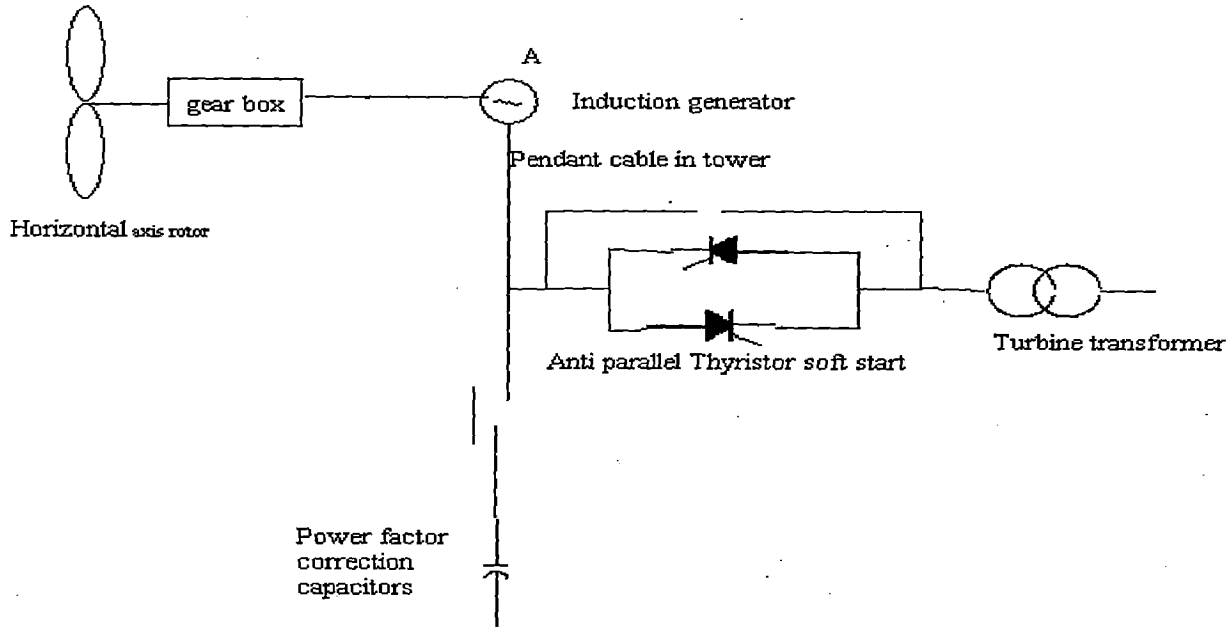

Fig.2.1 Schematic diagram of fixed speed turbine

2.2.2 Photo Voltaic

Photovoltaic power cells are solid state semi conductor devices that convert sunlight into direct current electrical power and the amount of power generated is directly related to the intensity of the light PV systems are most commonly used for stand alone applications and are commercially available with capacities ranging between one kW to one MW. The systems are commonly used in India and can contribute a great deal for rural areas, especially remote and inaccessible areas. High initial cost is a major constraint to large-scale application of SPV systems. R&D work has been undertaken for cost reduction in SPV cells, modules, and systems besides improvements in operational efficiency.

2.2.3 Bio mass

Biomass refers to renewable energy resources derived from organic matter, such as forest residues, agricultural crops and wastes, wood, wood wastes that are capable of being converted to energy. The extraction of energy from biomass is split into three distinct categories, solid biomass, biogas, and liquid bio-fuels. Biogas is obtained by an aerobically digesting organic material to produce the combustible gas methane. There are two common technologies, one of fermentation of human and animal waste in specially designed digesters, the other of capturing methane from municipal waste landfills [4].

2.3 Nonrenewable technologies

2.3.1 The Internal Combustion Engine

The most important instrument of the DG systems around the world has been the Internal Combustion Engine. Though the diesel engine is efficient, starts up relatively quickly, it is not environment friendly and has high operating and maintenance costs. Consequently its use in the developed world is limited. In India, the diesel engine is used widely on account of the immediate need for power, especially in rural areas, with out much concern either for long-term economics or for environment.

2.3.2 Combined Heat and Power Plant (CHP)

A CHP plant is an installation where there is simultaneous generation of usable heat and power (usually electricity) in a single process. The basic elements of a CHP plant comprise one or more prime movers usually driving electrical generators, where the heat generated in the process is utilized via suitable heat recovery equipment for a variety of purposes including: industrial processes, community heating and space heating.

CHP can provide a secure and highly efficient method of generating electricity and heat at the point of use. Due to the utilization of heat from electricity generation and the avoidance of transmission losses because electricity is generated on site, CHP typically achieves a 35 percent reduction in primary energy usage compared with power stations and heat only boilers. This can allow the host organization to make economic savings where there is a suitable balance between the heat and power loads.

2.3.3 Fuel Cells

Fuel cells produce direct current electricity using an electromechanical process similar to battery as a result of which combustion and the associated environmental side effects are avoided. Natural gas or coal gas is cleaned in a fuel cell and converted to a hydrogen rich fuel by a processor or internal catalyst. The gas and the air then flow over an anode and a cathode separated by an electrolyte and thereby produce a constant supply of DC electricity, which is converted to high quality AC power by a power conditioner.

2.3.4 Micro-turbines

Micro turbines are essentially very small combustion turbines, individually of the size of a refrigerator, that are often packaged in multiunit systems. In most

configurations, the micro turbine is a single-shaft machine with the compressor and turbine mounted on the same shaft as the electric generator. With a single rotating shaft, gearboxes and associated parts are eliminated, helping to improve manufacturing costs and operational reliability. The rather high rotational speeds vary in the range from 50,000 to 120,000 rpm, depending on the output capacity of the micro turbine. This high-frequency output is first rectified and then converted to 50 or 60 Hz [4].

2.4 Types of hybrid power system

A common hybrid system for the application in developing countries generally consists of the following main components:

1. A primary source of energy, i.e. a renewable energy resource;
2. A secondary source of energy for supply in case of shortages, i.e. a diesel generator set;
3. A storage system to guarantee a stable output during short times of shortages;
4. A charge controller;
5. Installation material (safety boxes, cables, plugs, etc.);
6. The appliances (lighting, TV/radio, etc.).

Hybrid systems are applied in areas where permanent and reliable availability of electricity supply is an important issue. Maintaining high availability with renewable energies alone usually requires big renewable energy generators, which can be avoided with hybrid systems. At favorable weather conditions, the renewable part of the system satisfies the energy demand, using the energy surplus to load the battery. The batteries act as "buffers", maintaining a stable energy supply during short periods of time, i.e. in cases of low sunlight or low wind. Moreover, the battery serves to meet peak demands, which might not be satisfied by the renewable system alone. A charge controller regulates the state of load of the battery, controlling the battery not to be overloaded. The complementary resource produces the required energy at times of imminent deep discharge of the battery, at the same time loading the battery.

Advantages of Hybrid Power Systems

- Provide Dependable, Utility-Grade 24 Hour AC or DC Power
- Not Dependent On Single Source Of Energy
- Flexible, Expandable, Able To Meet Changing Loads

- Simple, Quick, Low Cost Installation
- Low Operating Costs (O&M and Diesel Fuel)
- Simple Operation, Low Maintenance & Service Requirements
- User Not Required To Operate, Maintain, or Repair
- Lower Life-Cycle Cost Of Electricity For Remote Applications

Disadvantages of Hybrid Power Systems

- High Capital Cost Compared To Diesel Generators
- Diesel And Hybrids Have Very Different Cost Components
- More Complex than Stand-Alone Power Systems
- Requires Battery Storage and Power Conditioning
- Not Yet In Full Commercial (High Volume) Production ... Few Suppliers

2.4.1 PV/Diesel

Combining Photovoltaic arrays and a diesel generator set provides a rather simple solution and is feasible for regions with good solar resources. PV/Diesel hybrid systems require a DC/AC-inverter if appliances need alternating current, since PV modules provide direct current. Compared to the common solution for rural off grid electrification using diesel generator set alone, the hybrid solution using photovoltaic offers great potential in saving fuel. Experiences show annual fuel savings of more than 80% compared to stand-alone mini-grids on diesel generator set basis, depending on the regional conditions and the design of the system.

Naturally, the observed fuel saving varies over the year. The solar generator can provide about 100% of the electricity during summertime, while in winter this figure is less. Typically, in climatic regions like Germany a PV/Diesel hybrid system is designed to provide around 50% of the electricity from photovoltaic during winter, the rest being supplied with the diesel generator set.

2.4.2 Wind/Diesel

Wind/Diesel combinations are, in principal, built up in the same way as are PV/Diesel systems. From a perspective of financial competitiveness, they can be applied in regions where average wind speed is around 3.5 m/s already. If wind speed is sufficient, the wind turbine is in charge of the provision of energy. During short periods of time with low winds, the battery maintains a stable system, being replaced by the diesel generating set when low winds occur over longer periods of time.

Wind/Biogas

The concept of a Wind/Biogas system is to some degree similar to Wind/Diesel hybrid systems. Instead of the diesel generator set, here engine generator sets, small gas turbines, or some kinds of fuel cells can be used to generate electricity in addition to the wind turbine. The engine is fuelled by biogas, which is produced in an anaerobic digester. If the production of biogas is at times not sufficient, conventional gases as propane can be used instead. Wind or PV systems offer an environmental benign approach towards rural electrification.

Hydropower Hybrid Systems

Wind/Large Hydropower

On a seasonal basis, the two resources wind and hydropower tend to complement each other to some extent. Especially in winter, when river flows are low, wind has the potential to take over electricity supply. However, during late summer, both resources might become low, and the combination of both is then disadvantageous. Moreover, while hydro generators on rivers are usually at lower levels, wind resources are better at high elevations. For constant electricity generation, another energy resource would therefore be necessary. Since the combination of wind and hydropower offers just limited advantages, it is unlikely that these resources are combined in a project in developing countries, since this opportunity does not seem economically attractive. However, for some locations the situation might be different, so that the feasibility of Wind/Large Hydropower systems needs to be assessed for each case individually.

Wind/Micro-Hydro and PV/Micro-Hydro

While hybrid systems with large-scale hydropower generators seem unattractive, micro hydropower is more feasible. Micro-hydroelectric generators are turbines that are able to operate under low elevation head or low volumetric flow rate conditions, being suitable for small rivers. Where rivers have inconsistent flow characteristics (dry in summer, frozen in winter), a hybrid system applying wind or PV support can be attractive. A careful assessment of water resources is therefore essential.

Chapter 03
MATHEMATICAL MODELING OF HYBRID POWER SYSTEM

3.1 Wind Energy Conversion System

A schematic diagram of a wind energy conversion system is presented in the next section along with a detailed description of wind turbine and its modeling. The functionality of other system components is also discussed briefly. The functional structure of a typical wind energy conversion system is as shown in Figure 3.1.1,

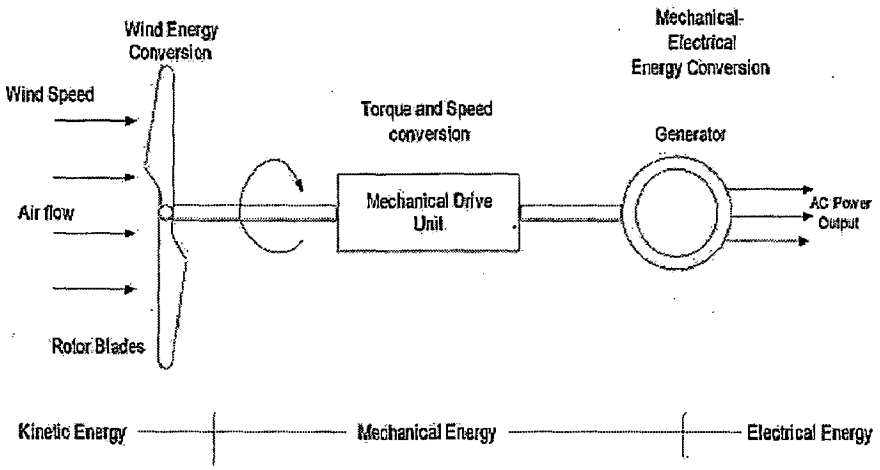

Fig 3.1.1: wind energy conversion system

A wind energy conversion system is a complex system in which knowledge from a wide array of fields comprising of aerodynamics, mechanical, civil and electrical engineering come together. The principle components of a modern wind turbine are the tower, the rotor and the nacelle, which accommodates the transmission mechanisms and the generator. The wind turbine captures the wind's kinetic energy in the rotor consisting of two or more blades mechanically coupled to an electrical generator. The main component of the mechanical assembly is the gearbox, which transforms the slower rotational speeds of the wind turbine to higher rotational speeds on the electrical generator side. The rotation of the electrical generator's shaft driven by the wind turbine generates electricity, whose output is maintained as per specifications. in this thesis induction generator is used as the generator for electrical power generation. Two distinctly different design configurations are available for a wind turbine, the horizontal axis configuration and the vertical axis configuration. The

vertical axis machine has the shape of an egg beater, and is often called the Darrieus rotor after its inventor. However, most modern turbines use horizontal axis design. In this chapter the dynamic model of a horizontal axis turbine is developed and simulated in the VisSim, as noted above, a WECS is a complex system converting wind energy to rotational energy and then to electrical energy. The output power or torque of a wind turbine is determined by several factors like wind velocity, size and shape of the turbine, etc. [5]

Wind/Diesel combinations are, in principal, built up in the same way as are PV/Diesel systems. From a perspective of financial competitiveness, they can be applied in regions where average wind speed is around 3.5 m/s already. If wind speed is sufficient, the wind turbine is in charge of the provision of energy. During short periods of time with low winds, the battery maintains a stable system, being replaced by the diesel generating set when low winds occur over longer periods of time.

The power and the torque generated by the wind turbine are as follows: [6]

$$P_{wind} = 0.5\rho\pi R_{bld}^2 C_p V_{wind}^3 \tag{3.1}$$

$$T_{wt} = \frac{P_{wind}}{\omega_{r-l}} \tag{3.2}$$

Where:

ρ = density of air

R_{bld} = swept area of the blade

C_p = performance coefficient

V_{wind} = wind speed.

T_{wt} = mechanical torque (at low speed shaft)

P_{wind} = output power of the turbine

W_{r-l}= rotor speed of the wind turbine - low speed shaft.

A typical C_p curve is shown in Figure 3.1.2. This characteristic defines C_p as a function of the tip-speed ratio (*TSR*) given by the equation 3:

$$TSR = \frac{\omega_{r-l} R_{bld}}{V_{wind}} \tag{3.3}$$

Where R_{bld} is the Radius of the wind turbine rotor

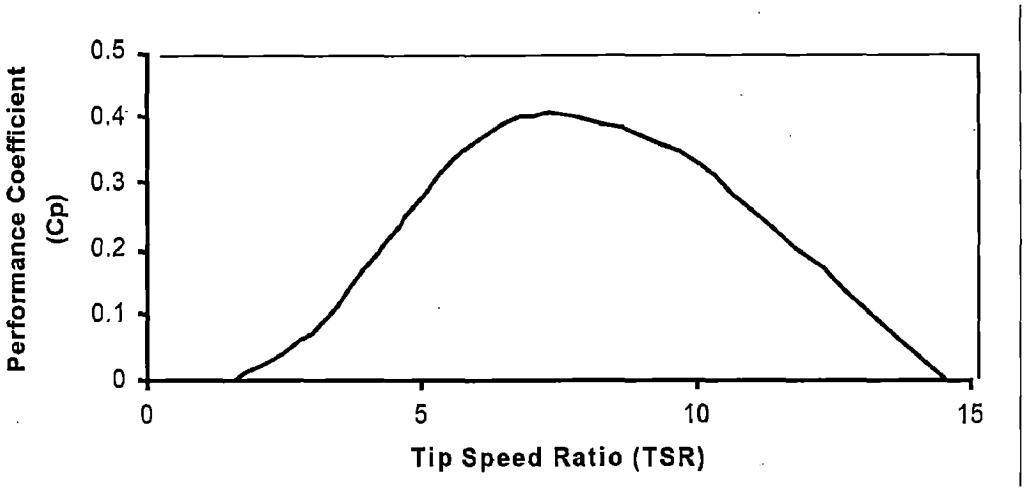

Figure 3.1.2: A typical Cp versus tip-speed ratio curve

As shown in Figure 3.1.3, the performance coefficient (*Cp*), which represents the efficiency of the wind turbine, varies as the wind speed increases. As the wind speed increases, the *TSR* decreases and the *Cp* increases until it reaches the maximum *Cp* at *TSR* = 7.8 (which corresponds to about 8 m/s for this wind turbine). As the wind speed continues to increase, the performance coefficient *Cp* declines. This process makes the wind turbine self-regulate its output power by operating at lower efficiency at high wind speed.

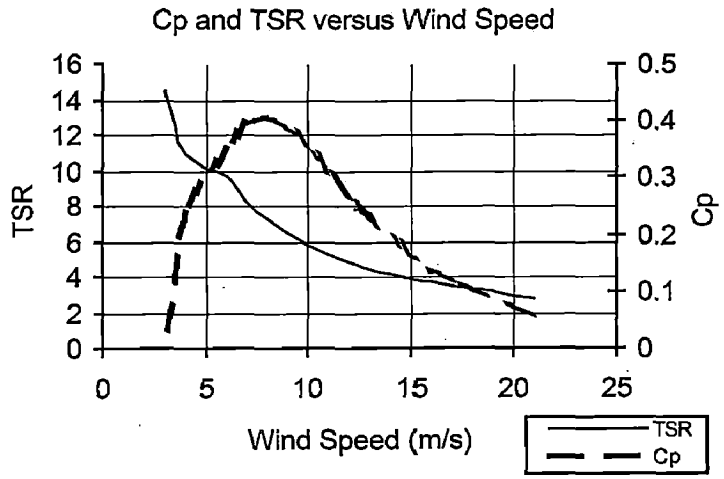

Figure 3.1.3: Cp and TSR as a function of wind speed for a fixed-speed turbine.

3.1.1 Wind speed data

The wind speed data used in this work has generated with the use of export block and slider gain which is shown in fig.3.1.4 and which are available in the simulation software VisSim 6.0 and we have to save that data in a file format for further use in work space. For the calculation of wind power we will use the data which were already stored in a specified file (.txt) format with the help of import block. The wind data used in this work is shown in fig. 3.1.5

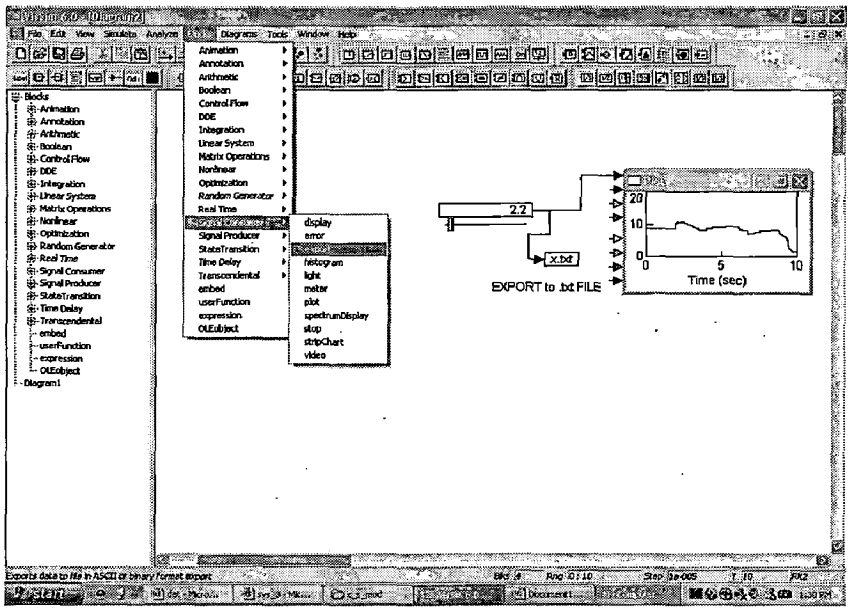

Fig.3.1.4: exporting data to .txt file

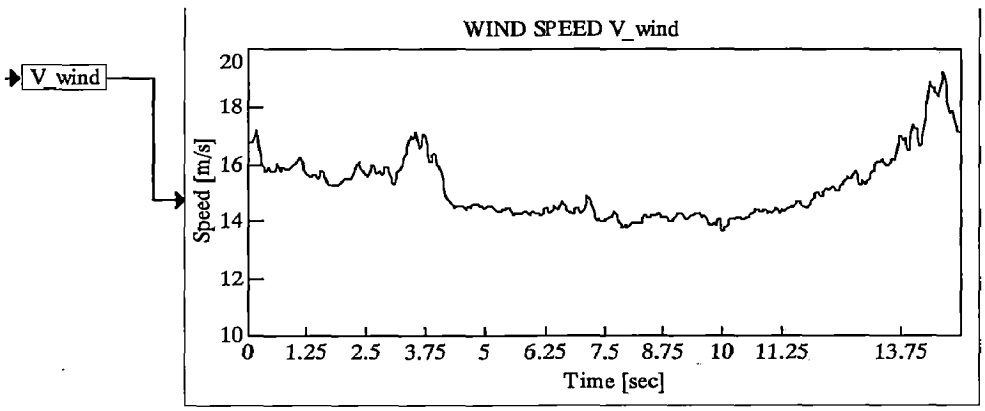

Fig 3.1.5: Wind data used in the simulation work

3.1.2 AC Wind Turbine [7]-[11]

In Figure 3.1.6, we show a single-line diagram of a hybrid power system where we dot-framed the portion of the diagram representing the AC WT. As shown in this figure, the WT consists of two machines: (1) a wind turbine and (2) an

asynchronous generator. In addition, the PFC capacitor (although not shown at this presentation level) and the line impedance R+jX are also included.

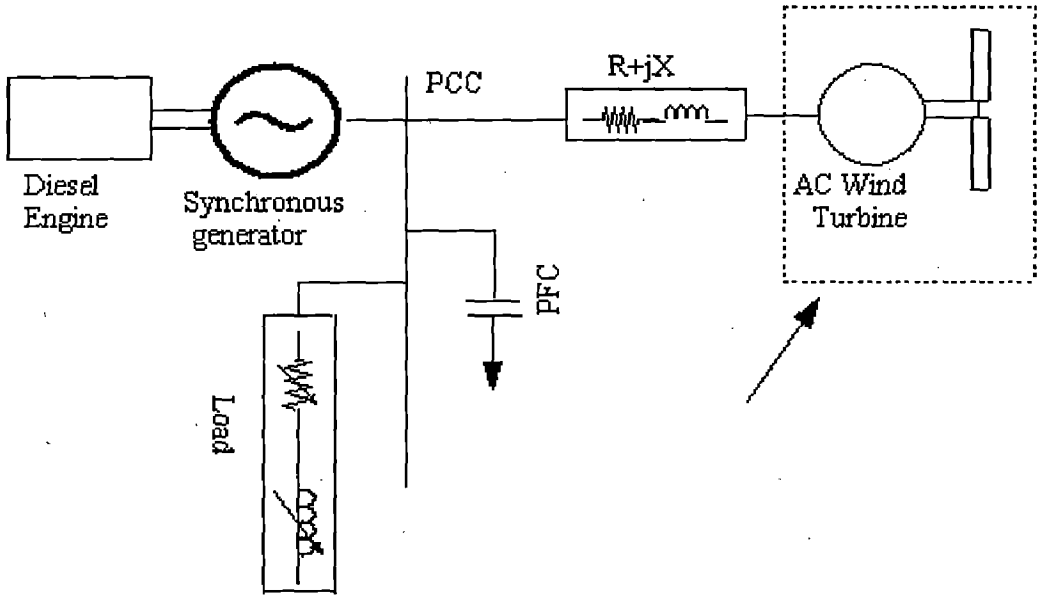

Figure 3.1.6: A single-line power system diagram with the WT module dot-framed

Figure 3.1.7 presents the top-view block diagram of the AC WT module implemented by the file wtg_base_mod.vsm. It consists of two blocks, shown in Figure 3.1.7(b), which are WT, and wind speed. The WT module has two outputs labeled kW and kVAR, which make the real and reactive power available for monitoring. In Figure 3.1.7(c), we present the expansion of the WT block, showing the interconnections of its principal components and their inputs and outputs. In this simulation, the reactive power has two components: (1) one absorbed by the induction generator and (2) one contributed by the PFC capacitor block.

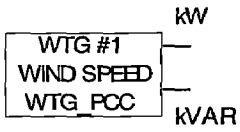

(a)

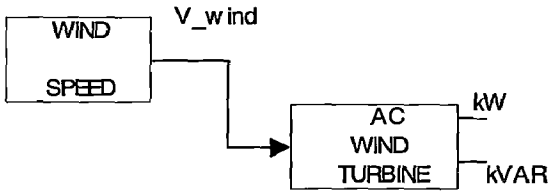

(b)

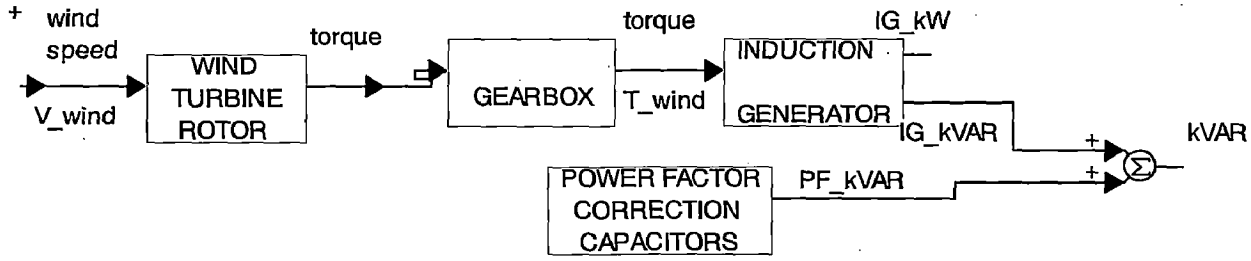

(c)

Figure 3.1.7: AC WT module implemented by the file wtg_base_mod.vsm: (a) top-view diagram, (b) second-level diagram, and (c) expansion of the AC WT block.

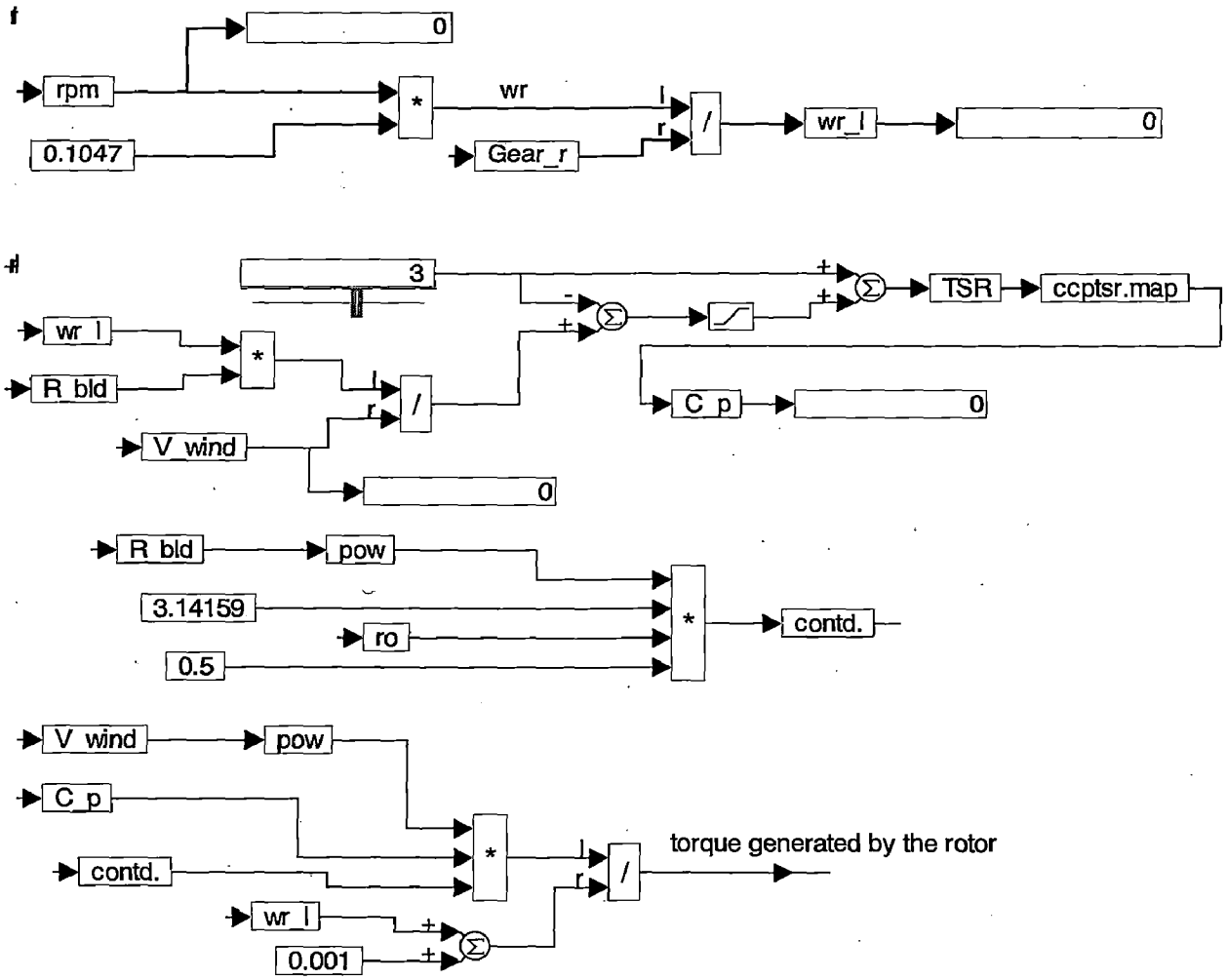

Figure 3.1.8: Simulation diagram of the wind turbine rotor

By clicking the mouse on any of the blocks shown in Figure 3.1.7(c), we obtain its lower level expansion. Such expansion of the wind turbine rotor block consists of: (1) the parameter module and (2) the simulation diagram. The parameter module contains two parameters: the air density ρ and the blade radius R_{bld}. By clicking the mouse on the simulation diagram, we can retrieve its expansion as shown in Figure 3.1.8. In the simulation diagram the velocity rpm of the induction machine is converted to the angular velocity ω_r in radians/second, which in turn is divided by the gear ratio $Gear_r$. This results in the angular velocity of the blade ω_{r_l}, which is given in equation 3.4, i.e., [6]

$$\omega_{r\_l} = \frac{\omega_r}{Gear_r} = \frac{0.1047 rpm}{Gear_r} \tag{3.4}$$

Then, the tip-speed ratio *TSR* is calculated using the relation and given in the equation (3.3)

$$TSR = \frac{\omega_{r-l} R_{bld}}{V_{wind}}$$

The nonlinear relation between *TSR* and the performance coefficient C_p is encapsulated in the map block, which performs piecewise linear interpolated look-ups. An ASCII data file is used for this mapping. The C_p, generated by the map block is then used to calculate the wind power P_{wind}, from which the torque generated by the wind turbine T_{wt} is determined. These calculations, shown in Figure 3.1.8, are represented by the following equations: (3.1)-(3.2)

$$P_{wind} = 0.5\rho\pi R_{bld}^2 C_p V_{wind}^3$$

$$T_{wt} = \frac{P_{wind}}{\omega_{r-l}}$$

3.1.3 Gearbox

In Figure 3.1.9, the expansion of the gearbox block is shown, in which the gear ratio is declared and the high-velocity torque is calculated, appended with a negative sign for future calculations, and denoted by T_{wind}.

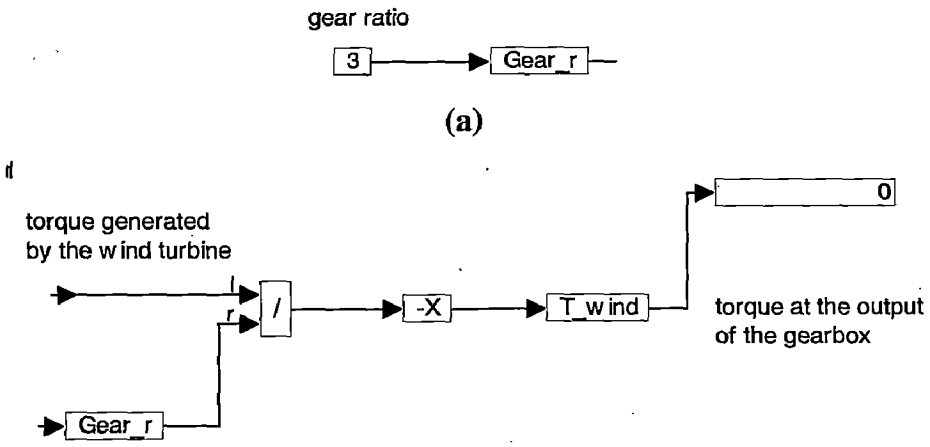

Figure 3.1.9: Gearbox: (a) parameter module expansion and (b) expansion of the simulation diagram

3.1.4 Induction Machines [12]-[14]

Most electric machines used as the prime mover in industry are induction motors. By its nature, an induction machine is an inductive load. Either as a motor or generator, this machine absorbs reactive power. The reactive power absorbed by the

induction machine comes from the line to which it is connected. In a hybrid power, the reactive power comes from the synchronous generator of the diesel generator set. In a wind turbine generator, a fixed capacitor is usually installed to supply some of the reactive power needed by the induction generator. The equivalent circuit of an induction machine connected to a power system is given in Figure 3.1.10. The power system is represented by the infinite bus Es and reactance Xs which represents the line impedance.

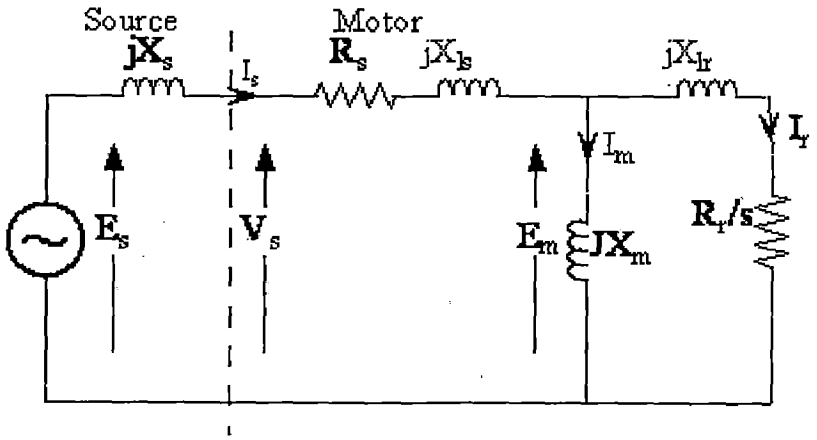

Figure 3.1.10: Equivalent circuit of an induction machine connected to power system.

Figure 3.1.11 shows the first-level expansion of the induction generator block. The parameters of the machine are listed in the parameter module as shown in Figure 3.1.11(a). In addition, the calculations of a set of constants in terms of these parameters, which simplify the simulation of induction generator, are also placed in the parameter module. This part of the parameter module is not shown in Figure 3.1.11(a). The following equations (3.5)-(3.7), implemented in the parameter module, specify these constants.[12]

$$a^{-1} = 1 + X'_{lr} / (X_m + X_{ls}), \qquad (3.5)$$

$$b^{-1} = 1 + X_{ls} / (X_m + X'_{lr}) \qquad (3.6)$$

$$c = \frac{r_s \omega_b}{X_{ls}}, \quad d = \omega_b, \quad e = \frac{r'_r \omega_b}{X'_{lr} X}, \quad f^{-1} = X_{ls}, \quad g^{-1} = X'_{lr}, \quad h = \frac{P}{2J\omega_b}, \quad k = \frac{3P}{4\omega_b} \qquad (3.7)$$

Where $\omega_b = 377$ (in radians per second or rad/sec) is the base speed.

The first-level expansion of the simulation diagram of the induction machine is shown in Figure 3.1.8(b). Let us concentrate on the two main blocks labeled ds_axis and qs_axis. Clicking the mouse will bring up the expansions of these blocks. They implement the following equations [(3.8)-(3.17)] describing the induction machine:

$$\Psi_{qs} = \omega_b \int [v_{qs2} - \frac{\omega}{\omega_b}\Psi_{ds} + \frac{r_s}{X_{ls}}(\Psi_{mq} - \Psi_{qs})]dt \tag{3.8}$$

$$\Psi_{ds} = \omega_b \int [v_{ds2} - \frac{\omega}{\omega_b}\Psi_{qs} + \frac{r_s}{X_{ls}}(\Psi_{md} - \Psi_{ds})]dt \tag{3.9}$$

$$\Psi'_{qr} = \omega_b \int [v'_{qr} - \frac{\omega - \omega_r}{\omega_b}\Psi'_{dr} + \frac{r'_r}{X'_{lr}}(\Psi_{mq} - \Psi'_{dr})]dt \tag{3.10}$$

$$\Psi'_{dr} = \omega_b \int [v'_{dr} - \frac{\omega - \omega_r}{\omega_b}\Psi'_{qr} + \frac{r'_r}{X'_{lr}}(\Psi_{md} - \Psi'_{dr})]dt \tag{3.11}$$

$$\Psi_{mq} = a\Psi'_{qr} + b\Psi_{qs} \tag{3.12}$$

$$\Psi_{md} = a\Psi'_{dr} + b\Psi_{ds} \tag{3.13}$$

$$i_{qi} = f(\Psi_{qs} - \Psi_{mq}) \tag{3.14}$$

$$i_{di} = f(\Psi_{ds} - \Psi_{md}) \tag{3.15}$$

$$i'_{qr} = g(\Psi_{qr} - \Psi_{mq}) \tag{3.16}$$

$$i'_{dr} = g(\Psi_{dr} - \Psi_{md}) \tag{3.17}$$

where v_{qs2} and v_{ds2} are defined in the PFC Capacitor block described below.

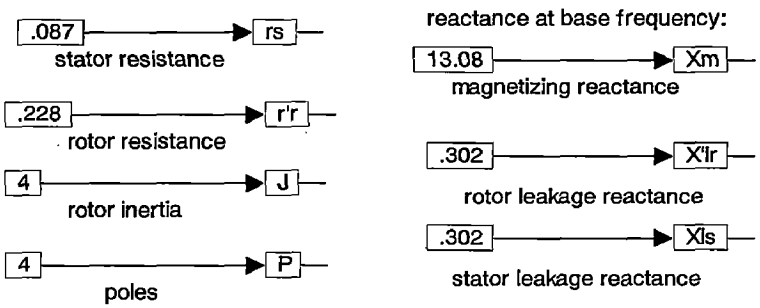

(a)

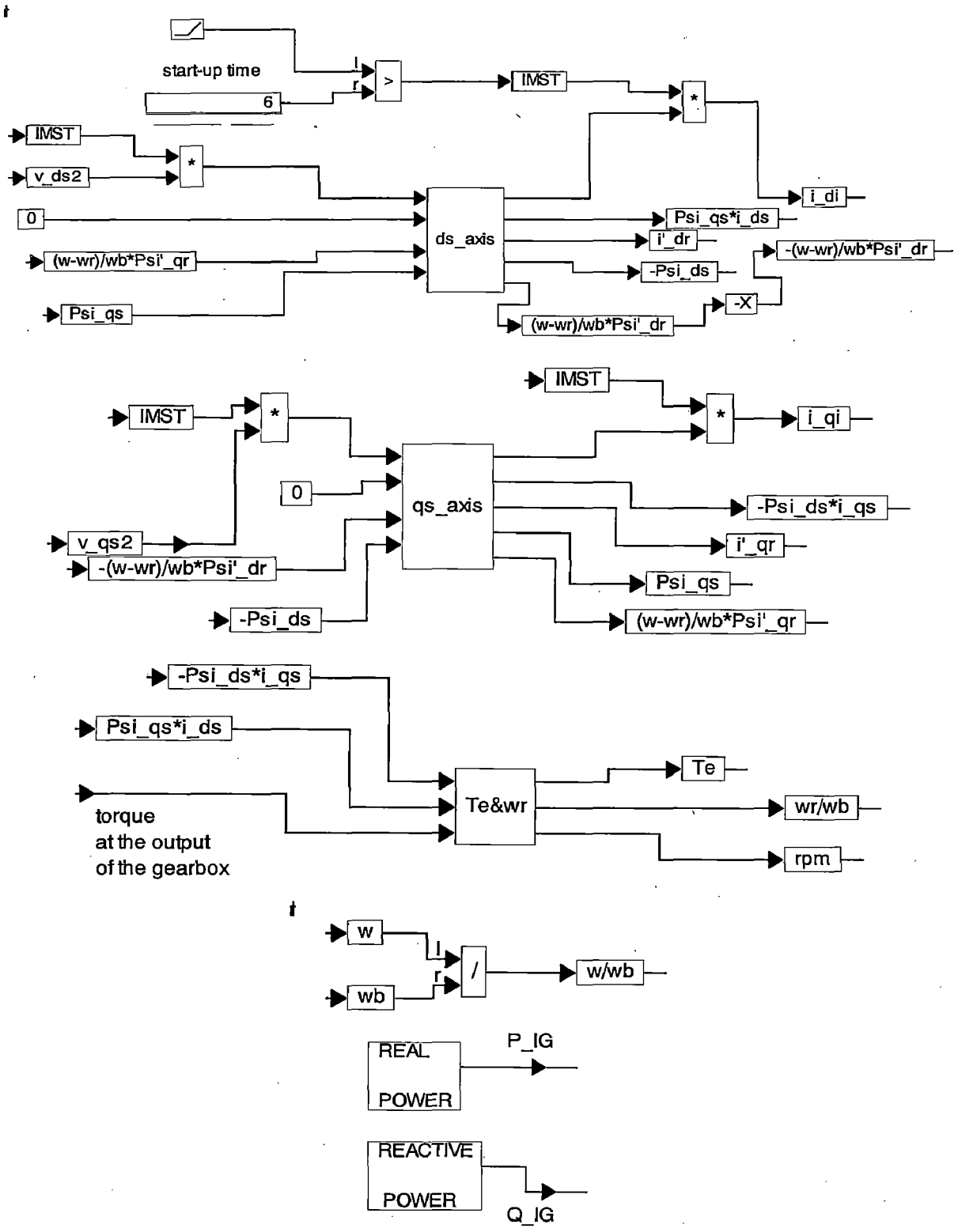

(b)

Figure 3.1.11: First-level expansion of the induction generator block:
(a) Parameter module and (b) Simulation diagram.

Note that according to the model assumed (as best seen in Figure 3.1.9) the induction generator current components, i_{di} and i_{qi}, equal to the respective transmission line

currents, i_{ds} and i_{qs}, minus the respective components, i_{dPFC2} and i_{qPFC2}, of the PFC capacitor current. The block labeled Te&wr implements the following equations [(3.18)-(3.20)]:

$$T_e = k(\Psi_{ds} i_{qi} - \Psi_{qs} i_{di}) \tag{3.18}$$

$$\frac{\omega_r}{\omega_b} = h\int (T_e - T_{wind})dt \tag{3.19}$$

$$rpm = 9.54929\frac{\omega_r}{P/2} \tag{3.20}$$

The equation implemented in the real power block is given in (3.21)

$$P_{IG} = 3\times 10^{-3}(v_{qs2} i_{qi} + v_{ds2} i_{di})\,[\text{kW}] \tag{3.21}$$

The equations [(3.22)-(3.23)] implemented in the reactive power block are

$$Q_{IG} = 3\times 10^{-3}(v_{qs2} i_{di} - v_{ds2} i_{qi})\,[\text{kVAR}], \tag{3.22}$$

$$S_{IG} = 3\times 10^{-3}\sqrt{v_{qs2}^2 + v_{ds2}^2}\sqrt{i_{qi}^2 + i_{di}^2}\ [\text{kVA}] \tag{3.23}$$

Figure 3.1.13 presents the PFC capacitor and transmission line model block. Its parameter module is expanded in Figure 3.1.13(a) and shows the following parameters C_{pf2} PFC capacitor at the wind turbine site

R_{LN} Transmission line resistance

L_{LN} Transmission line inductance.

The simulation diagram is expanded in Figure 3.1.13(b) and its corresponding circuit diagram is shown in Figure 3.1.12.

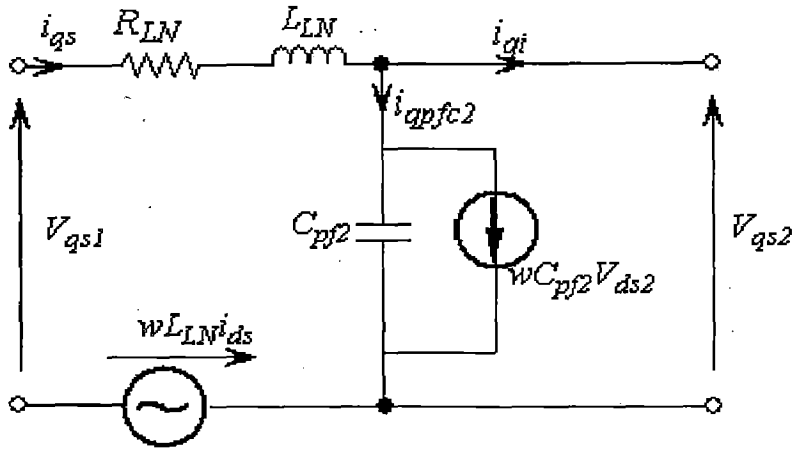

(a)

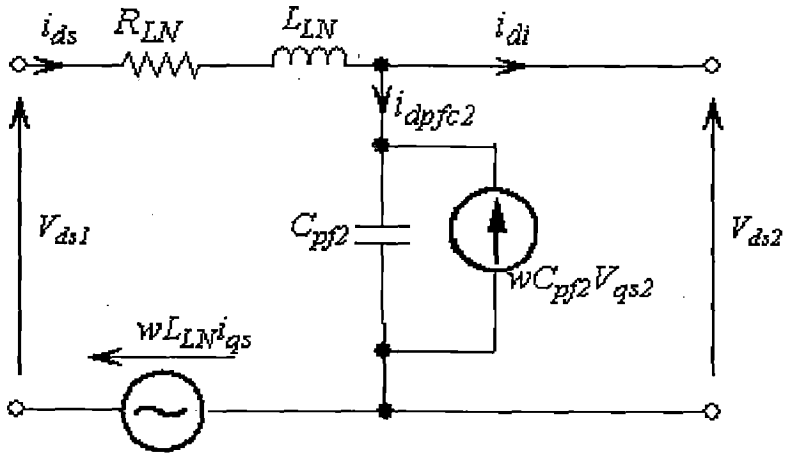

(b)

Figure 3.1.12: Circuit diagram of the PFC capacitors and transmission line model block: (a) q-axis circuit representation and (b) d-axis circuit representation

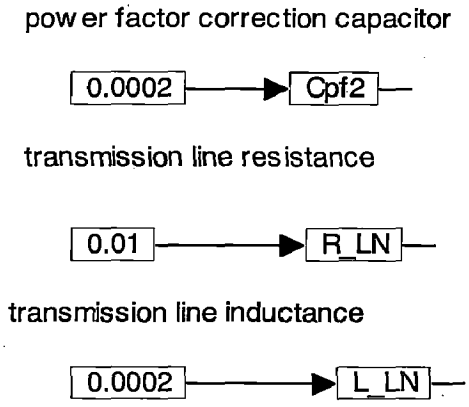

(a)

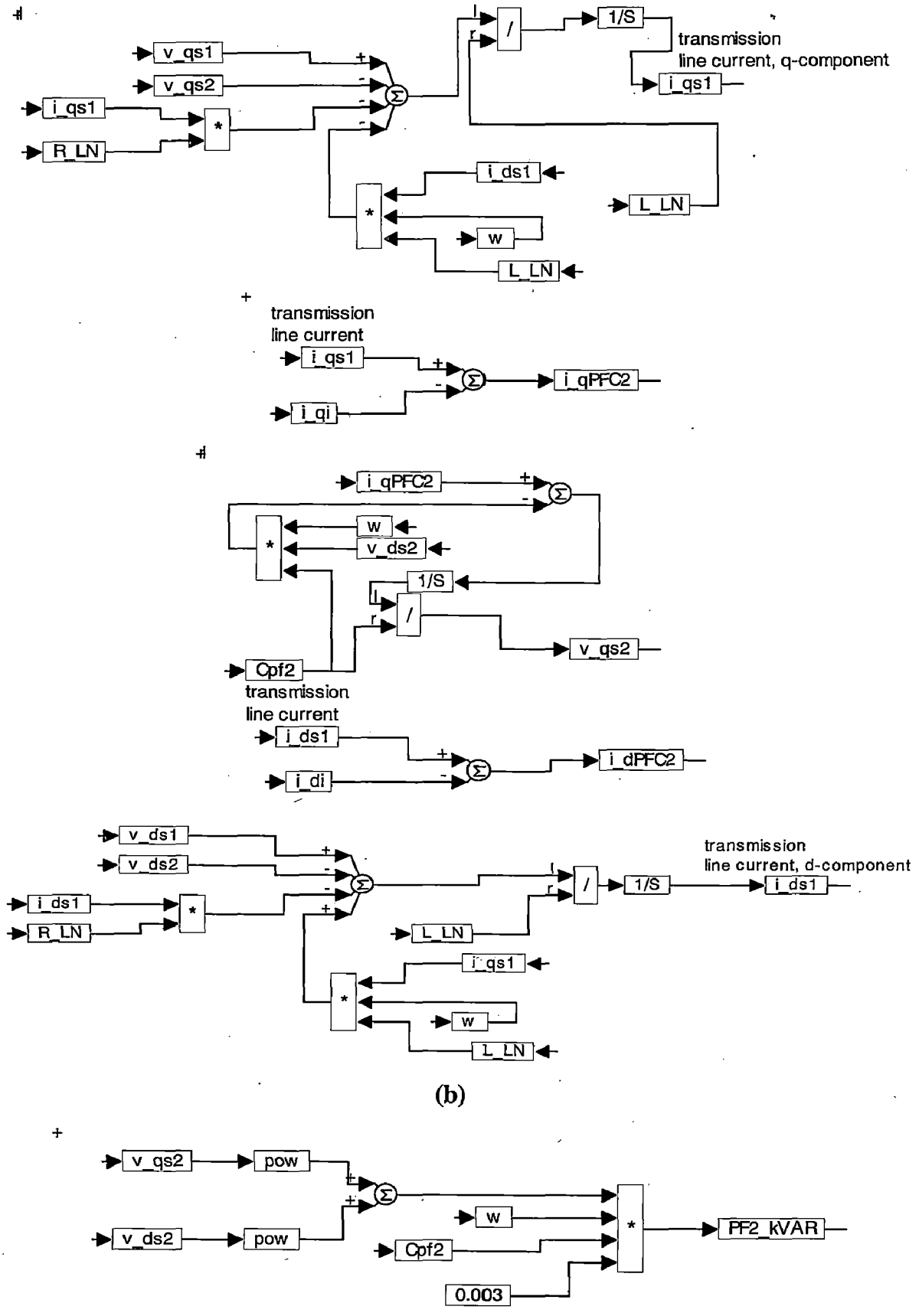

Figure 3.1.13: PFC capacitors and transmission line model block: (a) parameter module, (b) simulation diagram, and (c) expansion of the reactive power block.

The transmission line connects the diesel generator with the induction generator. According to the circuit diagram, the d-q axis equations [(3.24)-(3.29)] involved follow:

$$i_{qPFC2} = i_{qs1} - i_{qi} \tag{3.24}$$

$$i_{dPFC2} = i_{ds1} - i_{di} \tag{3.25}$$

$$v_{qs2} = \frac{1}{C_{pf2}} \int (i_{qPFC2} - \omega C_{pf2} v_{ds2}) dt \tag{3.26}$$

$$v_{ds2} = \frac{1}{C_{pf2}} \int (i_{dPFC2} + \omega C_{pf2} v_{qs2}) dt \,, \tag{3.27}$$

$$i_{qs1} = \frac{1}{L_{LN}} \int (v_{qs1} - v_{qs2} - \omega L_{LN} i_{ds1} - R_{LN} i_{qs1}) dt \,, \tag{3.28}$$

$$i_{ds1} = \frac{1}{L_{LN}} \int (v_{ds1} - v_{ds2} + \omega L_{LN} i_{qs1} - R_{LN} i_{ds1}) dt \tag{3.29}$$

Finally, Figure 3.1.13(c) shows the expansion of the reactive power block, which implements the equation given in (3.30)

$$PF2_{kVAR} = 3 \times 10^{-3} \omega C_{pf2} (v_{qs2}^2 + v_{ds2}^2) \tag{3.30}$$

3.2 Diesel Generator

In Figure 3.2.1, we show a single-line diagram of a hybrid power system where we dot-framed the portion of the diagram that represents the diesel generator. As shown in this figure, the system consists of two machines: (1) a diesel engine and (2) a synchronous generator.

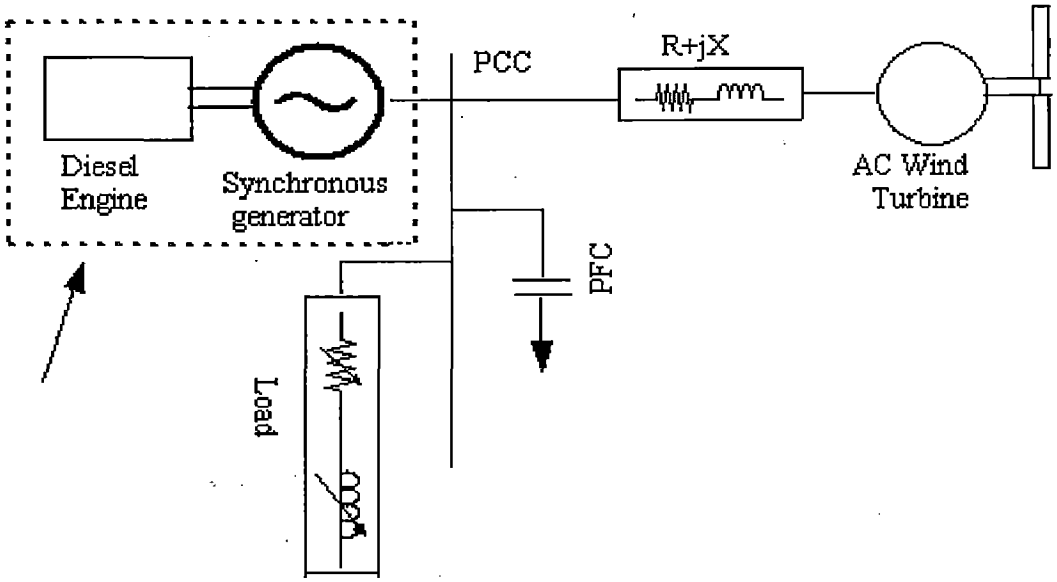

Figure 3.2.1: A single-line power system diagram with the DG portion dot-framed

3.2.1 Diesel Engine

Small diesel-power generating sets (diesel generator sets) have been the traditional way to address the problem of the lack of electricity. They provide a simple solution for rural electrification and can be designed for different capacities, being adapted to the needs of the consumers. In cases security of supply is not of major importance, single diesel generator sets can be applied for electrification, accepting that no electricity can be supplied in times the generator set is out of commission, i.e. due to repair or maintenance. This problem can be met by using a group of diesel generator sets, with the other generator sets providing backup. With diesel generator sets, the electric current is produced within the village itself. Diesel generator sets have problems with short durability, which is due to the fact that they work very inefficiently when running just at fractions of their rated capacity. Typically, the efficiency of operation is between 25-35%. Moreover, frequent start-up and shut-down procedures decrease their lifetime as well. Many, especially rural, areas are far away or isolated (i.e. islands) from higher developed regions so that the regular supply with diesel fuel becomes a logistical problem and an important financial burden even in countries, where fuel is heavily subsidized. Moreover, the transportation of diesel fuel can result in severe environmental damage, as experienced

Diesel engines are ubiquitous in society precisely because they are the most efficient and cost-effective prime mover available. This efficiency is primarily due to the high compression ratio that is used to create heat and cause spontaneous ignition of diesel fuel. Because they must be built to with stand the very high internal forces of high compression, diesel engines cost more than other engines. Greater fuel efficiency, reliability, and longevity justify the extra cost.

There is a correlation between the amount of fuel burned per unit of work and the exhaust emissions an engine generated. The diesel engine is inherently more fuel efficient than gasoline engines. Therefore, certain exhaust emissions, including those that are routinely tested for in emissions, including those that are routinely tested for in emissions tested modeled on regulated emissions are lower for diesel engines than for a gasoline engine of comparable age, condition and capability. These regulated emissions include total hydrocarbon (THC), carbon monoxide (CO) and nitrogen oxide (NO_x). This is true even if the diesel engine is not fitted with a catalytic converter and the gasoline engine is fitted with a catalytic converter. Greater fuel efficiency that reduces the amount of fuel required, required CO_2 emissions compared to gasoline engines, and reductions in regulated emissions explains why the diesel engine is considered to be a more environmentally acceptable engine than the gasoline engine in the world.

Figure 3.2.2(a) represents the top-view diagram of the DG module. Two outputs—SD_{kW} and SD_{kVAR} —make the real and reactive power available for monitoring with either a display or plot block. Clicking the mouse will bring up the second-level block diagram, such as the one in Figure 3.2.2(b), which represents the principal functional blocks of the diesel generator with their interconnections and in which all inputs and outputs are clearly shown. According to the block diagram in Figure 3.2.2(b), the speed control block generates a proper fuel/air ratio (represented by the variable %fuel) for the diesel engine. This enables the engine to generate the proper torque to drive the synchronous generator. The voltage regulator (with the proper adjustment of the field current of the synchronous generator) controls the line voltage V_s.

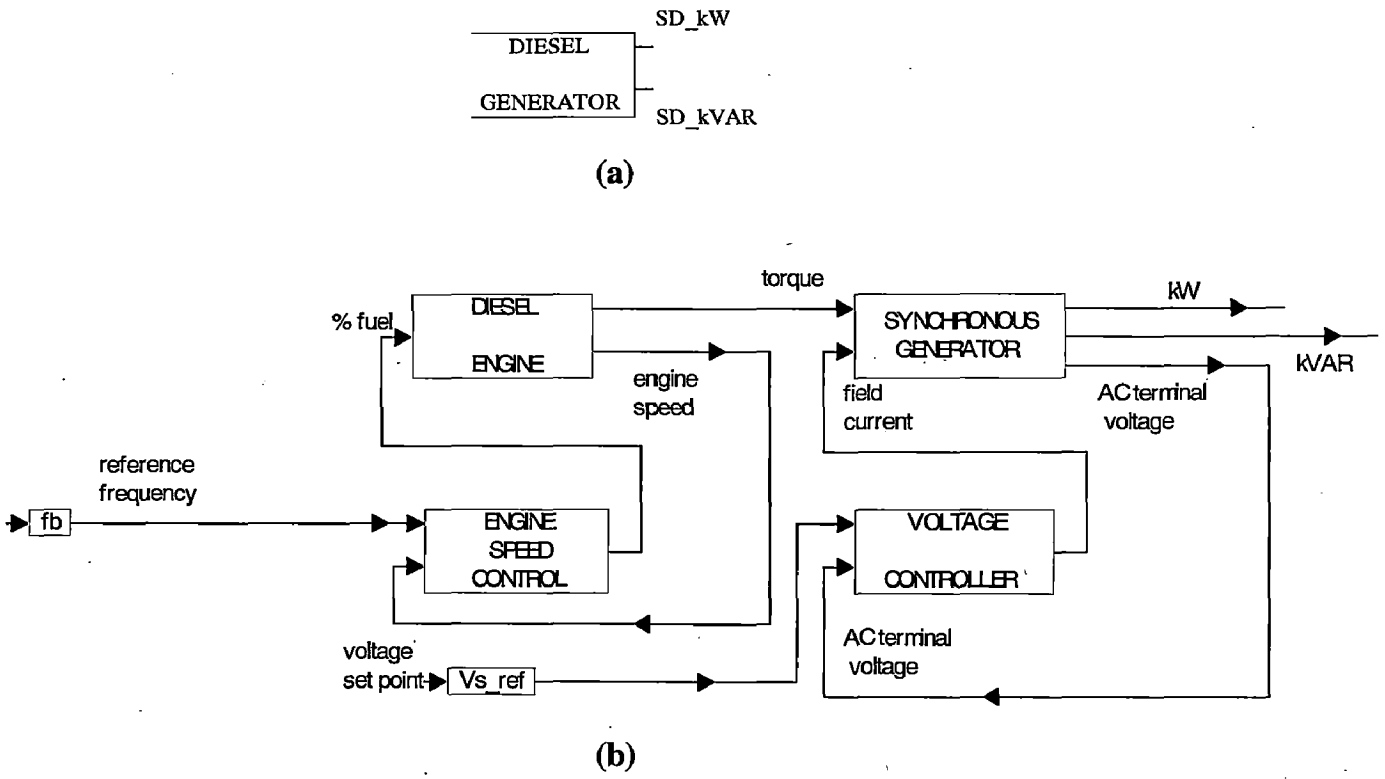

Figure 3.2.2: Block diagrams of the DG module: (a) top-view and (b) second-level showing principal functional modules and their interconnections

Figure 3.2.3 represents a simple simulation diagram of a diesel engine. Its POWER=f($\%_{FUEL}$) characteristic is represented as a straight line with the slope and the minimum value of the $\%_{FUEL}$

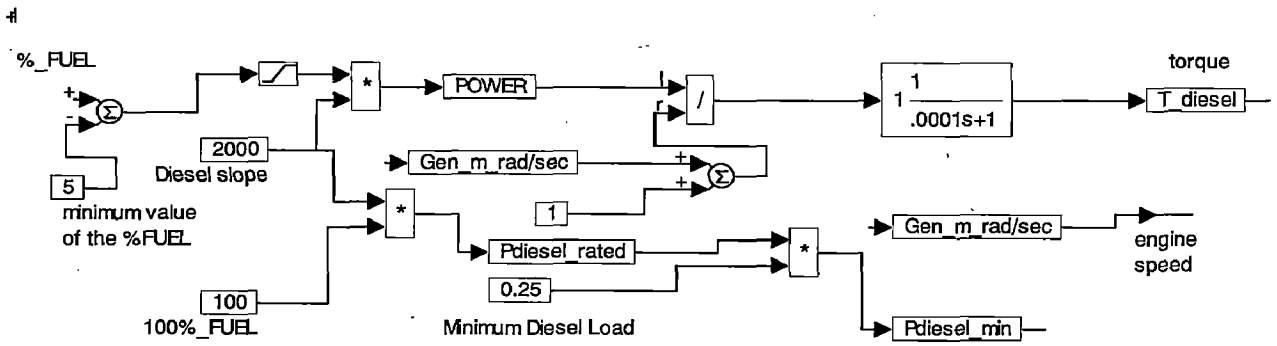

Figure 3.2.3: Simulation diagram of the diesel engine module

As it can be seen in Figure 3.2.3, the rated power for the simulated diesel engine is 200 kW. Using the generated power and angular velocity $Gen_{m\_rad/sec}$, the torque T_{diesel} is generated assuming the first-order dynamics. The minimum diesel load P_{diesel_min} (chosen in Figure 3.2.3 as 25% of the rated power) is calculated. The first- and

second-level expansions of the synchronous generator module are shown in Figure 3.2.4. The first level, presented in Figure 3.2.4(a), consists of two compound blocks (parameter module and simulation diagram) and shows two control inputs—T_{diesel} and the field current i_f—and three outputs—SD_{kW} , SD_{kVAR} , and V_s. Note that for clarity of presentation, the output V_s is calculated in the PCC module as shown in Figure 2.4(c). Figure 3.2.4(b) lists all machine parameters used in this work.

3.2.2 Synchronous Generator [15]-[17]

Figure 3.2.4(c) shows the first-level expansion of the synchronous generator simulation diagram with the following compound blocks: torque equation, power calculations (where the outputs SD_{kW} and SD_{kVAR} are generated), and the Q-generator and the D-generator. This block diagram also shows that the electromotive force generated is assumed as a reference (i.e., its phase is assumed to be zero). Consequently, its d-axis component is zero, which is symbolically shown as a zero input to the D-generator. Under this assumption, the input to the Q-generator is defined and given in equation (3.31):

$$E_{q\_D} = K_{e\_D}\omega\Phi = K_{e\_D}\omega L_f i_f \qquad (3.31)$$

where Φ is the flux proportional to the field current (i_f). The other parameters are explained in Figure 3.2.4(b). The Q-generator and D-generator, shown in Figure 3.2.5, generate the current i_{qSD} and i_{dSD}, respectively, contributed by the diesel generator to the system at the PCC module. These currents are calculated according to the following equations [(3.32) & (3.33)]:

$$i_{qSD} = \frac{1}{L_{qSD}}\int (E_{q\_D} - v_{qs1} - R_{SD}i_{qSD} - \omega L_{dSD}i_{dSD})dt, \qquad (3.32)$$

$$i_{dSD} = \frac{1}{L_{dSD}}\int (-v_{ds1} - R_{SD}i_{dSD} + \omega L_{qSD}i_{qSD})dt \qquad (3.33)$$

Figure 3.2.6(b) shows the power calculation block in an expanded form. The electrical power generated is calculated according to the following equation (3.34):

$$P_{Egen\_D} = 3\, i_{qSD}E_{q\_D}\,. \qquad (3.34)$$

Then the real power provided to the system is calculated and given in equation (3.35)

$$P_{gen} = 3(v_{qs1}i_{qSD} + v_{ds1}i_{dSD}) \text{ [W]} \quad \text{or} \quad SD_{kW} = 10^{-3}P_{gen} \text{ [kW]}. \tag{3.35}$$

The apparent power SD_{kVA} and the reactive power SD_{kVAR} are also calculated in this block according to the following equations (3.36) & (3.37):

$$SD_{kVA} = 3\times 10^{-3}\sqrt{v_{qs1}^2 + v_{ds1}^2}\sqrt{i_{qSD}^2 + i_{dSD}^2}\,, \tag{3.36}$$

$$SD_{kVAR} = 3\times 10^{-3}(v_{qs1}i_{dSD} - v_{ds1}i_{qSD})\,. \tag{3.37}$$

Finally, in Figure 3.2.6(a) the torque equation is simulated to obtain the angular velocity of the diesel generator $Gen_{m\_rad/sec}$. This brings us to the equation (3.38):

$$Gen_{m\_rad/\sec} = \frac{1}{J_{SD}}\int (T_{diesel} - T_{gen} - B_{SD}Gen_{m\_rad/\sec})dt\,, \tag{3.38}$$

where T_{gen} represents the generated electrical power P_{Egen_D}; i.e., and given in (3.39)

$$T_{gen} = \frac{P_{Egen\_D}}{Gen_{m\_rad/\sec}} \tag{3.39}$$

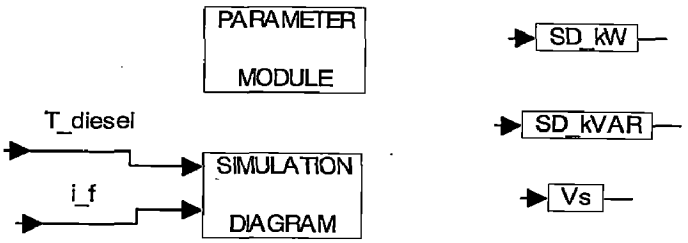

(a)

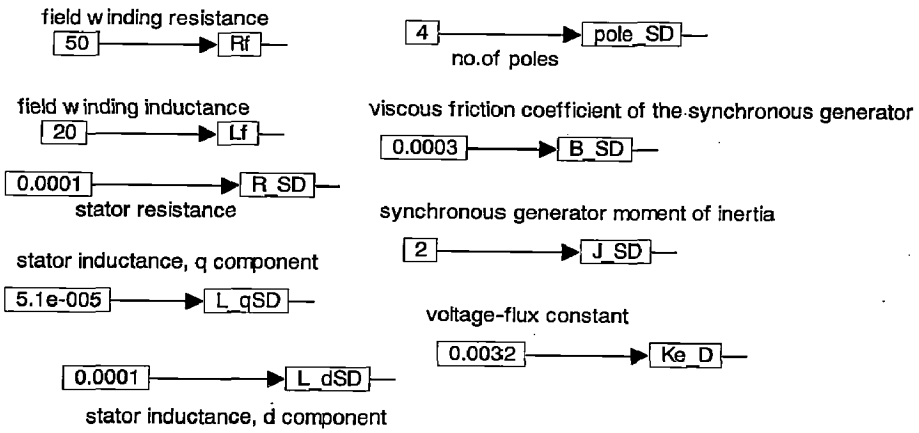

(b)

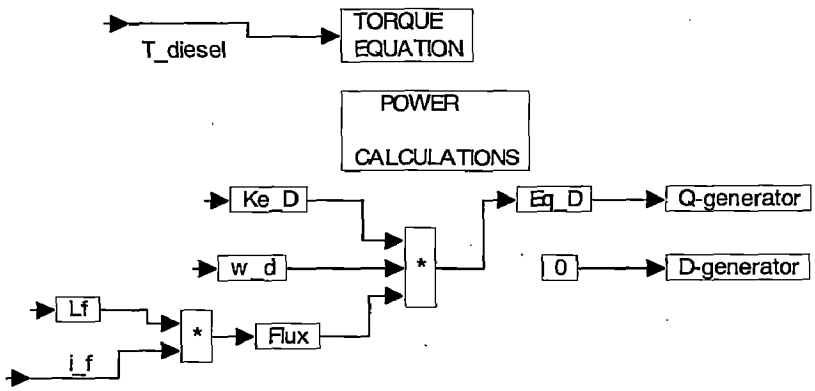

(c)

Figure 3.2.4: First- and second-level expansion of the synchronous generator module: (a) first-level expansion, (b) parameter module expansion, and (c) simulation diagram expansion

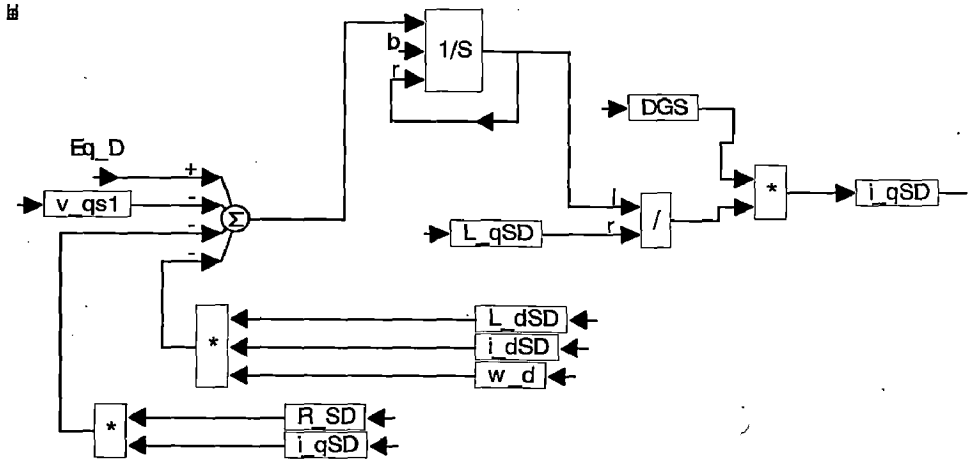

Q-Generator

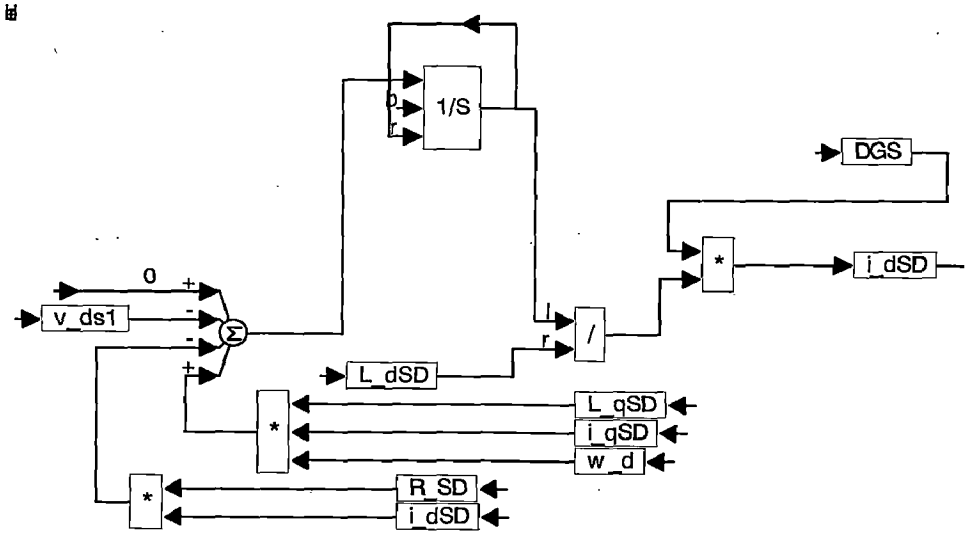

D-Generator

Figure 3.2.5: Simulation diagram of the synchronous generator (DG module): Q-generator and D-generator

3.2.3 Engine Speed Controller

Two more blocks in the second level simulation diagram of the diesel generator module are shown in Figure 3.2.2(b): the engine speed control block and the voltage regulator. They are fully expanded in Figures 3.2.7 and 3.2.8, respectively. In Figure 3.2.7, using the angular velocity $Gen_{m\_rad/sec}$, we find the value of the ratio f/f_{b_d} along with an important system variable, the angular frequency $\omega_d = 2\pi f$. Then the frequency f is found. The speed of the diesel engine is controlled by the control variable $\%_{FUEL}$ generated by the governor (represented in the simulation by the proportional + integral [PI] controller) so that the relative frequency error $1- f/f_{b\_d}$ is driven to zero.

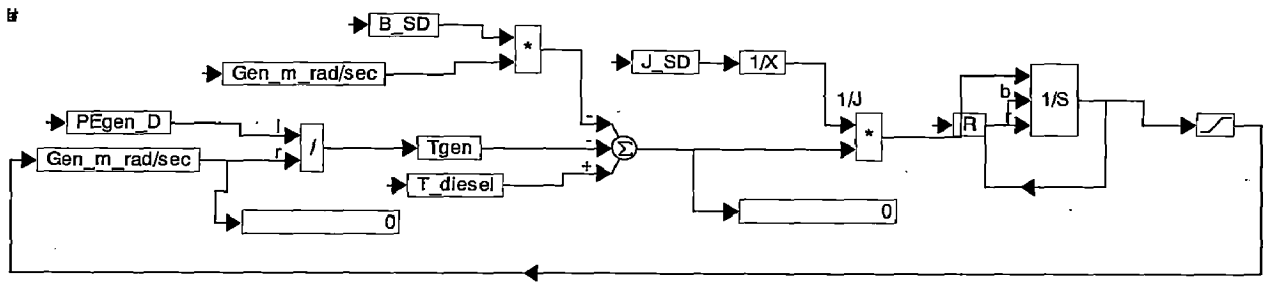

(a)

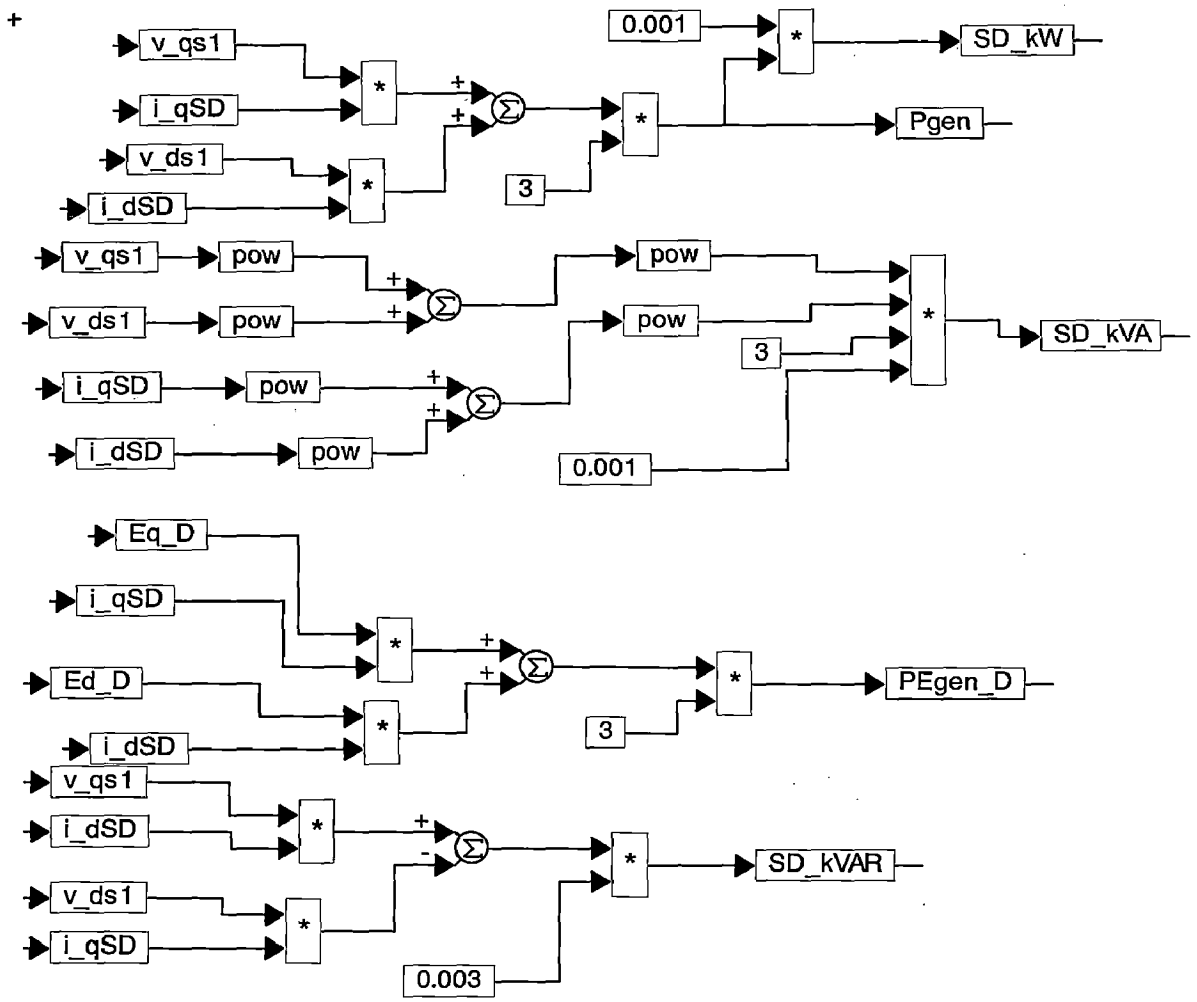

(b)

Figure 3.2.6: Simulation diagram of the synchronous generator (DG module): (a) Torque equation and (b) Power calculations

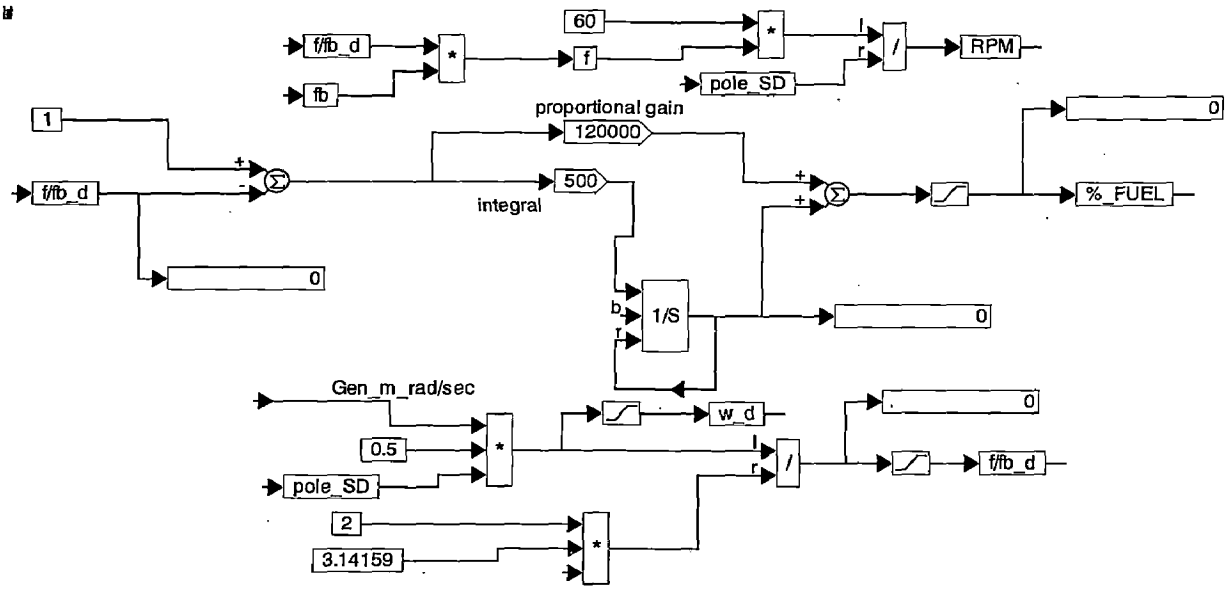

Figure 3.2.7: Simulation diagram of the engine speed control system

3.2.4 Voltage Controller

In Figure 3.2.8, the field current i_f of the synchronous generator is calculated according to the equation (3.40)

$$i_f = \frac{1}{L_f}\int (V_f - R_f i_f)dt, \tag{3.40}$$

Where the voltage V_f is defined as the output of the PI controller determined to drive the line voltage error $V_{s\_ref} - V_s$ to zero to drive to zero the error $V_{s\_ref} - Eq\_D$ during the synchronization process. To smooth the field current, the low-pass filter with the cut-off frequency of 20 rad/sec is added. We should adjust proportional and integral gain to avoid saturating the field current. The practical solution is to make proportional gain slightly smaller than $(V_f)/(V_{s\_ref})$ and then to set the largest possible integral gain to avoid saturation.

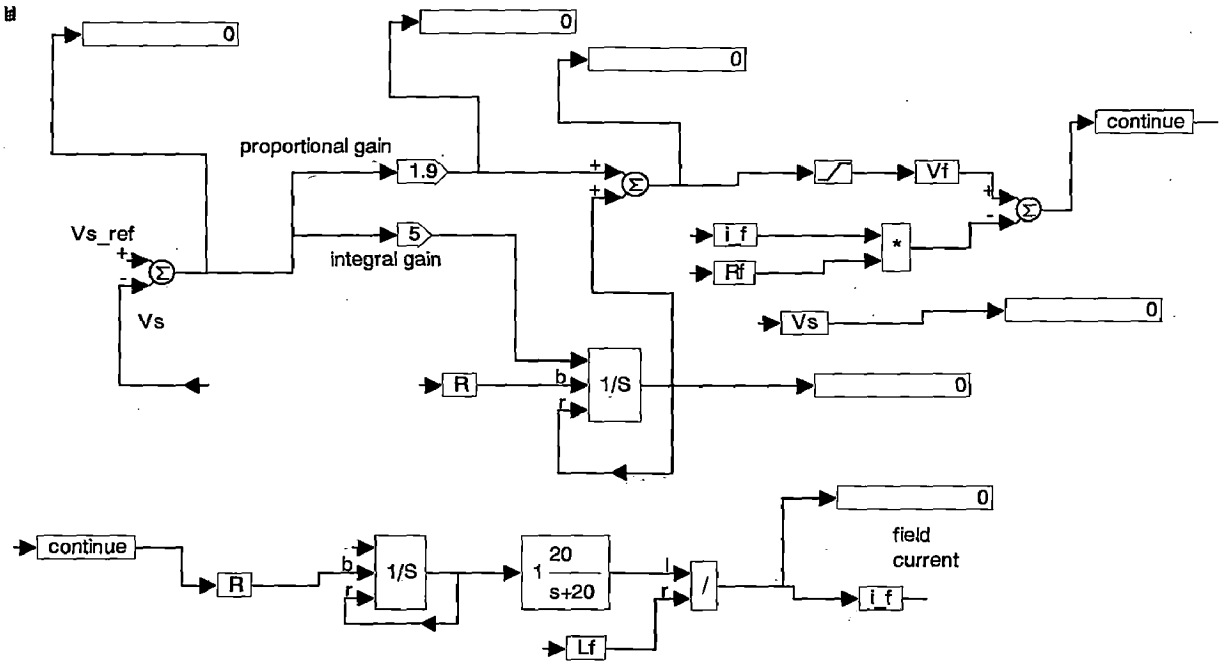

Figure 3.2.8: Simulation diagram of the voltage regulator

3.3 Wind diesel system [18]-[23]

Studies have shown that the integration of wind turbines into an autonomous diesel electric system (i.e., wind-diesel) can be economically viable, and that the potential market for wind-diesel is considerable. The advantage of hybrid power systems is the combination of the continuously available diesel power and locally available, pollution-free wind energy. With the hybrid power system, annual diesel fuel consumption can be reduced and pollution can be minimized at the same time. To

take full advantage of the wind energy when it is available and to minimize diesel fuel consumption, a proper control strategy must be needed to maintain the voltage and frequency with in the allowable limits. The control system is subject to the specific constraints of a particular application. It has to maintain power quality, measured by the quality of electrical performance, meaning that both the voltage and the frequency must be controlled. Wind energy offers the possibility of generating substantial amounts of energy. Consumer load is continuous and varies throughout the day. Power available from wind generator is variable due to fluctuating wind velocity. Wind-diesel hybrid systems are generally used for remote power supply. A power fluctuation problem has been experienced when the wind generator system uses an induction generator for energy conversion. This problem could be because of the turbulent nature of wind velocity, and the reactive power drawn by these induction generators.

A physical diagram of the system that was analyzed in this work is shown in Figure 1.

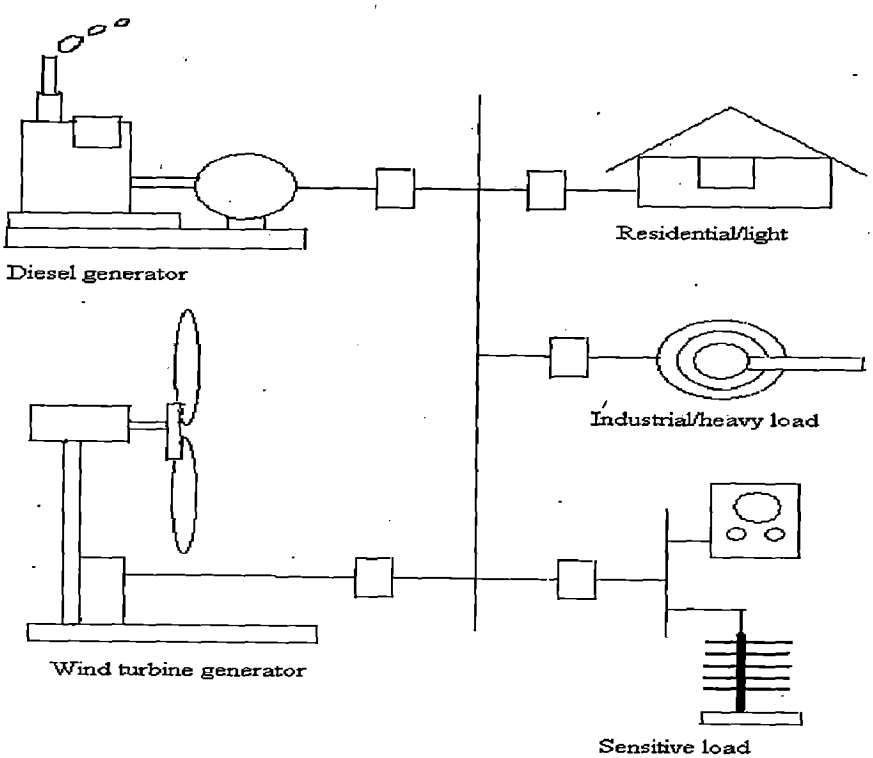

Fig 3.3.1: Physical diagram of the Hybrid power system

The wind turbine is operated with an induction generator to produce electrical power. The diesel engine is operated in parallel to supply the load. The local loads are mostly

residential and light loads. Other loads include water pumps, compressors, and other heavy equipment. The system has two types of generation: the diesel generator and the wind turbine generator (Fig.3.3.1). The diesel generator provides smooth generation, whereas the output power of a wind turbine generation depends on the wind velocity. The wind velocity is reflected in the power generation. For example, if the wind changes very smoothly, the output power of the wind turbine will also change very smoothly. On the other hand, wind turbulence causes the output power to fluctuate. In the power system network, the balance of active power and reactive power must be maintained. The diesel generator set, then, must be able to keep the power balanced when the wind turbine or local load varies.

Fig. 3.3.2 is a single-line diagram that represents the analyzed power system.

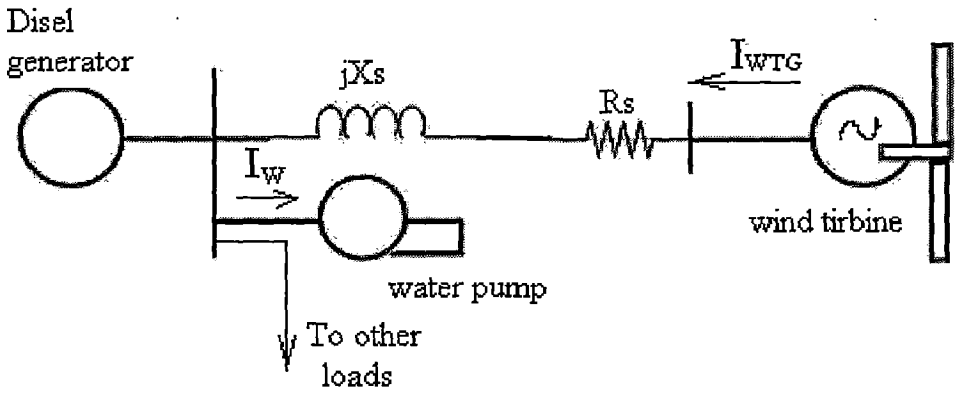

Fig 3.3.2: Single line diagram of the power system analyzed

- **Components of Power System**

The system we discussed in this work consists of three major subsystems:

- Diesel generator,
- Wind turbine generator, and
- Point of common coupling
- Load on the System

Already we have given the detailed explanation for the diesel generator module and AC Wind Turbine module, the following section explains the remaining components in the system (i.e. point of common coupling and load on the system)

3.3.1 Point of common coupling

The PCC module, the node where all power sources and power sinks are connected, must be included in every simulated case (i.e. two case studies). In Figure 3.3.3, we show a single-line diagram of a hybrid power system where dot-framed the PCC portion of the diagram [18]

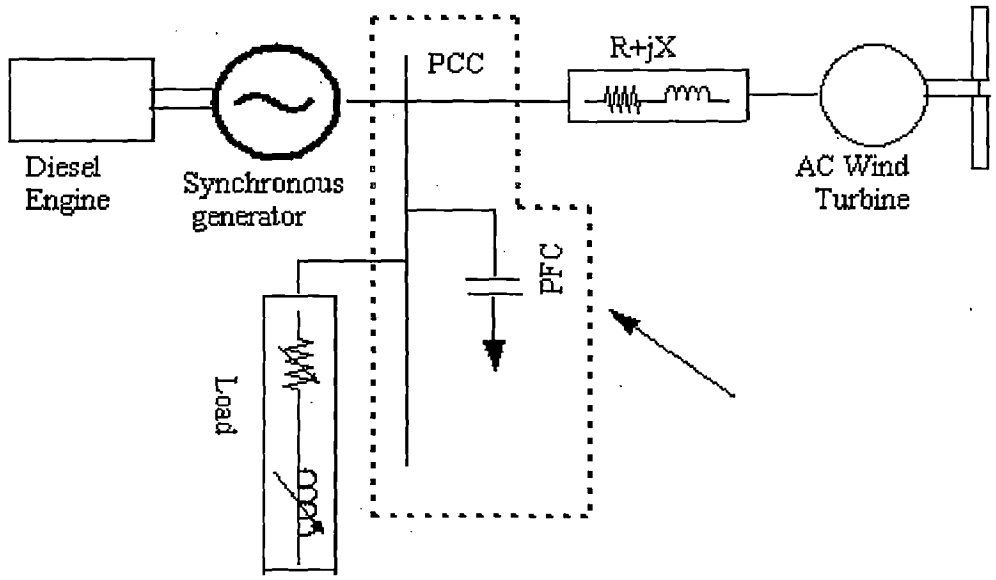

Figure 3.3.3: A single-line hybrid power system diagram with the PCC Portion dot-framed

To bring the PCC module to the simulation screen by using the Add command and selecting file PCC_m.vsm. Next, it obtains top-view diagram of the PCC module (shown in Figure 3.3.4) by clicking the mouse on the rectangle representing this module. This view features two elements: (1) the parameter module compound block; and (2) the simulation diagram compound block.

Figure 3.3.5, which is the expansion of the parameter module, shows the parameters that were used for the PCC. In addition, the base frequency w_b in rad/sec is calculated in this module. Figure 3.3.6 represents the expansion of the simulation diagram compound block. Recall that in all simulations we use the d-q axis convention. Therefore, each voltage and current has two components. Consequently, Figure 3.3.6(a) represents the relationship between the d-axis components of the currents of all system modules, and it shows how the d-axis component of the line voltage is obtained. The same is repeated in Figure 3.3.6(b) for the q-axis components. To make the relationships between the currents and voltages involved readily apparent, the

circuit diagrams (corresponding to the simulation diagrams of Figure 3.3.6) are shown in Figure 3.3.7.

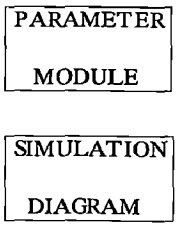

Figure 3.3.4: Top-view diagram of the PCC module

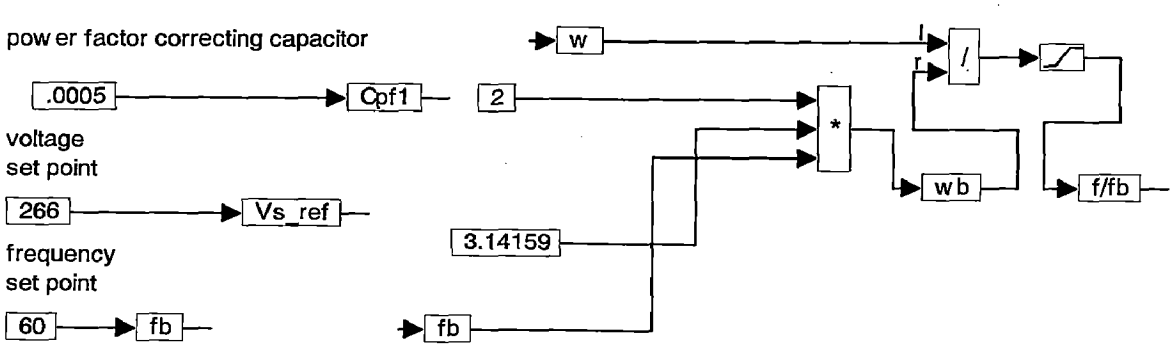

Figure 3.3.5: Parameter module of the PCC

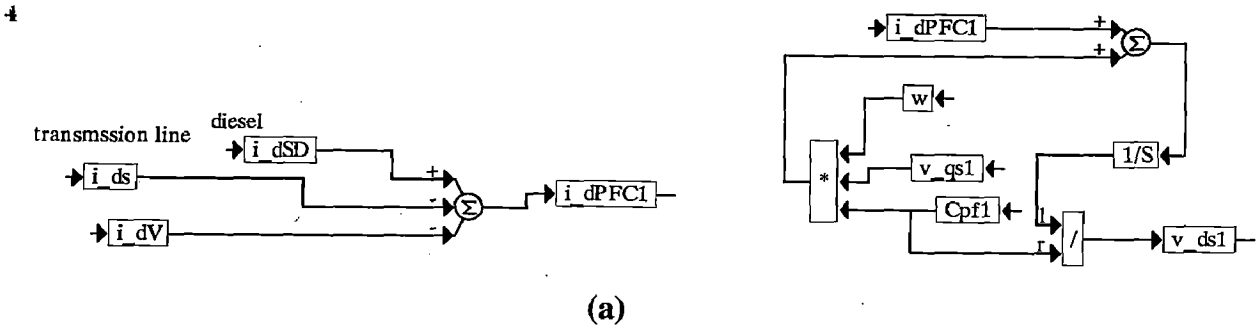

(a)

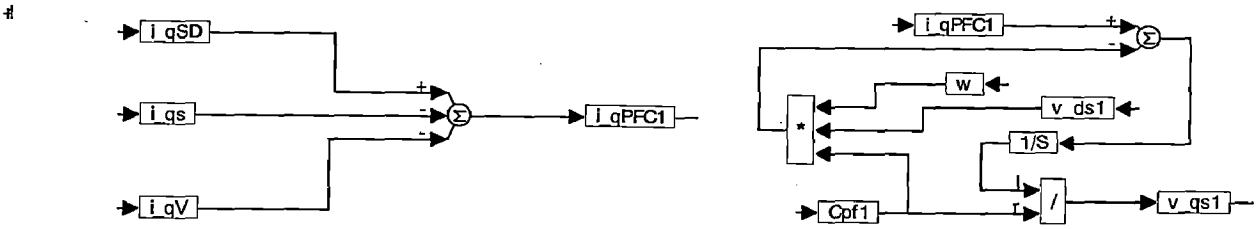

(b)

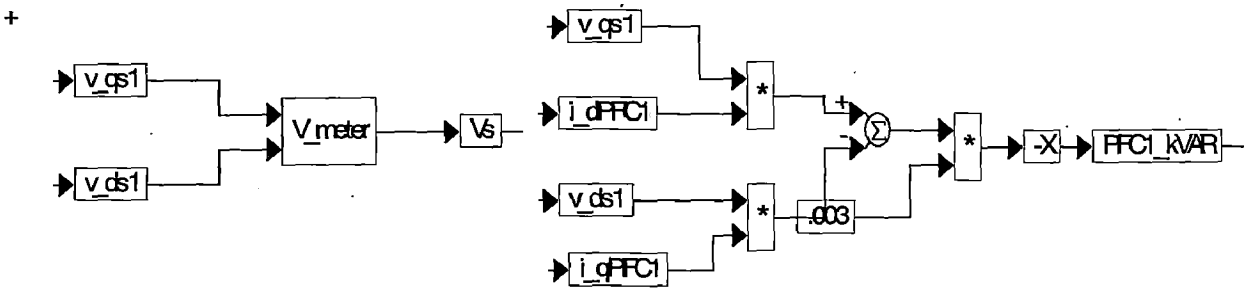

(c)

Figure 3.3.6: PCC module simulation diagram: (a) d-axis, (b) q-axis, and (c) Calculation of the system voltage and the reactive power generated by the PFC capacitors

Note that if the current representing a given module enters the top node in the circuit diagram of Figure 3.3.7 (or is added at the summing junction in Figure 3.3.6), its power is positive when it is generating power and negative when it is absorbing power. On the other hand, if the current representing a given module leaves the top node in the circuit diagram of Figure 3.3.7 (or is subtracted at the summing junction in Figure 3.3.6), its calculated power is positive when it is absorbing power and negative when it is generating power. To follow the general convention that the power generated is positive and the power absorbed is negative, we invert the sign of the power calculated for the modules represented by the currents leaving the top node in the diagram shown in Figure 3.3.7.

Let us consider some examples. The diesel generator always generates the real power. Therefore, its real power is always positive, or we say that it follows the assumed current sign convention. On the contrary, the diesel generator may generate or absorb the reactive power; the diesel reactive power may be positive or negative, depending on the load demand. The wind turbine generator during the motoring period absorbs real power, meaning that it draws the current from the PCC junction. The direction in which this current flows is the same as the direction assumed. Therefore, the calculated (absorbed) real power is positive. It requires the change of sign to follow the general convention. For the same reason, we must change the sign of the real power calculated when the wind turbine is generating. According to the circuit diagrams in Figure 3.3.7, we define the following currents and given in equations (3.41) & (3.42):

$$i_{qpfc1} = i_{qsd} - i_{qs} - i_{qv} \tag{3.41}$$

$$i_{dpfc1} = i_{dsd} - i_{ds} - i_{dv} \tag{3.42}$$

Using the same circuit diagram, we write the following equations (3.43) & (3.44) defining q-axis and d-axis components v_{qs1} and v_{ds1} of the line voltage (V_s):

$$v_{qs1} = \frac{1}{C_{pf1}} \int (i_{qPFC1} - \omega C_{pf1} v_{ds1}) dt \,, \tag{3.43}$$

$$v_{ds1} = \frac{1}{C_{pf1}} \int (i_{dPFC1} + \omega C_{pf1} v_{qs1}) dt \,, \tag{3.44}$$

Where C_{pf1} is the PFC capacitor of the value in the parameter module shown in Figure 3.3.5, and ω is the real system frequency calculated in the DG module that must be a part of every simulated power system. These equations are implemented in the right-side parts of Figure 3.3.6(a) and Figure 3.3.6(b).

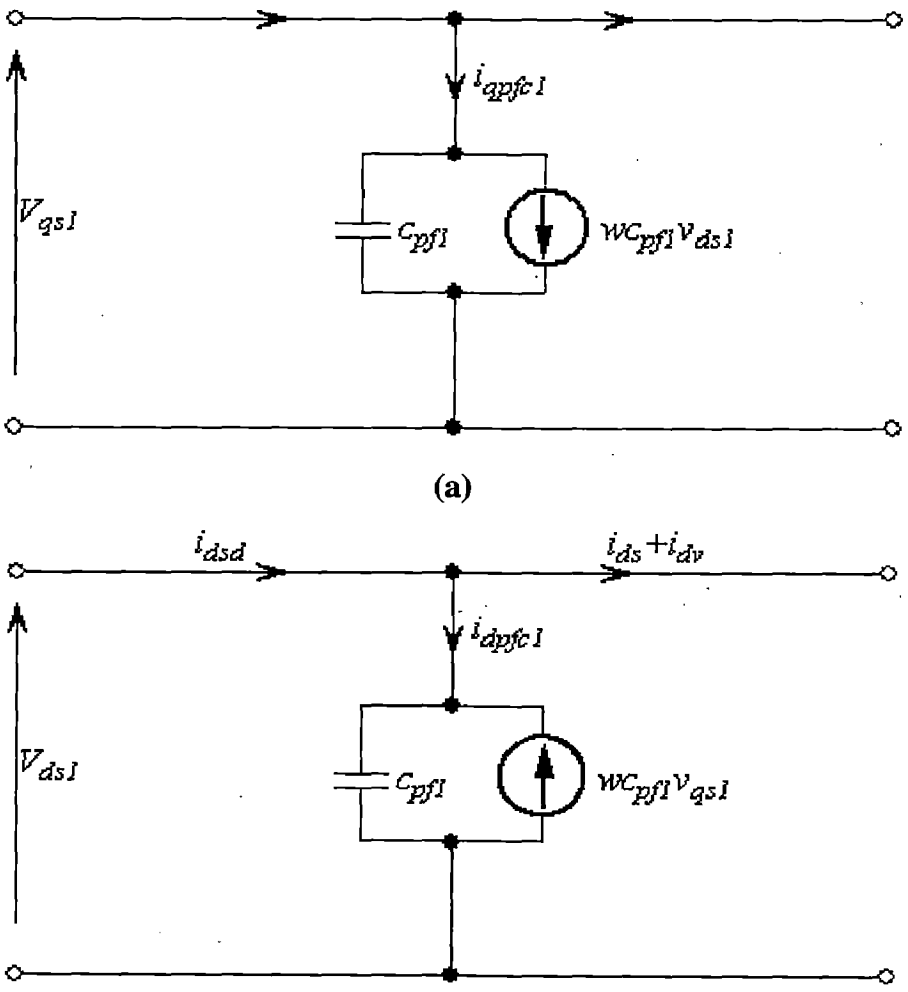

Figure 3.3.7: PCC module circuit diagram: (a) q-axis and (b) d-axis

V_s is calculated in the compound block V_meter, shown in Figure 3.3.6(c), according to the equation (3.45):

$$V_s = \sqrt{v_{qs1}^2 + v_{ds1}^2} \,. \tag{3.45}$$

The calculation of the reactive power generated by the PFC capacitor is also shown in Figure 3.3.6(c). According to our convention, the reactive power generated must be positive. If the power is generated, the currents i_{qPFC1} and i_{dPFC1} should be entering the summing junction. In other words, the calculated reactive power is negative, so we introduce the inversion of sign in the calculation of the reactive power shown in Figure 3.3.6(c).

3.3.2 Load on the System

Figure 3.3.8 represents a single-line diagram of a hybrid power system where dot-framed the portion of the diagram that represents the village load.

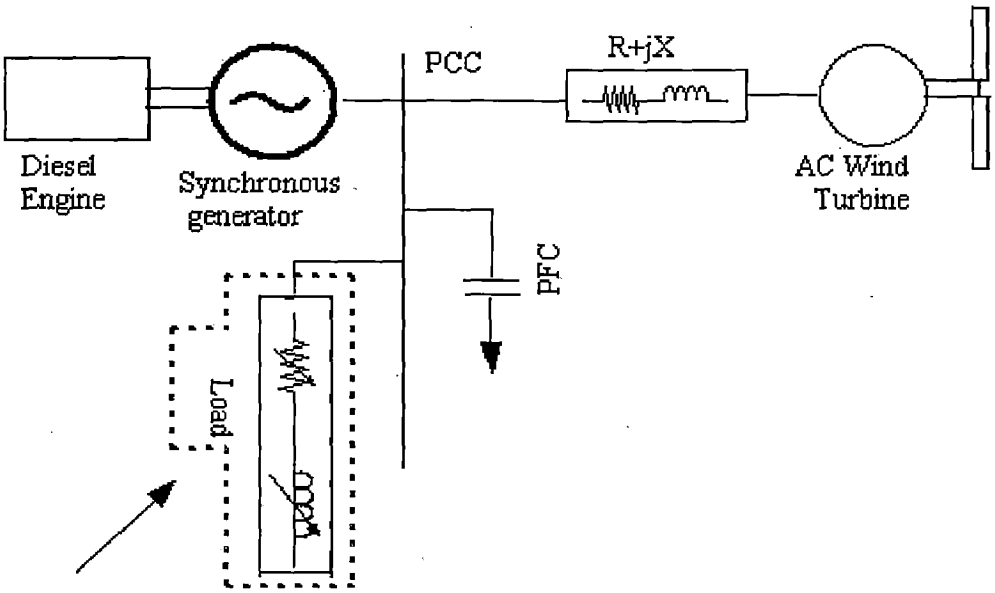

Figure 3.3.8: A single-line diagram of a hybrid power system with
The LOAD module dot-framed

Figure 3.3.9(a) represents the block diagram of the LOAD module as it appears in simulation diagrams. Its first-level expansion, shown in Figure 3.3.9(b), has two output variables, available for direct monitoring; i.e., the real power load P_V in [kW] and the reactive power load Q_V in [kVAR]. The expansion of its simulation diagram block is shown in Figure 3.3.9(c) and consists of three compound blocks: (1) power calculations, (2) q-axis, and (3) d-axis representations of the load. The output variables of the last two blocks are the component i_{qV} and i_{dV} of the load current. These current components enter the PCC node. The parameter module in the first-level expansion is further expanded in Figure 3.3.9(d). The parameters defined by the

us, specific to the application considered, are the rated real power consumption P_v and the power factor pf. We have a choice between fixed load, declaring the values of variables P_{v1} and pf_1, and the load profile, declaring P_{v2} and pf_2 in a form of time series. In Figure 3.3.10, we show an example of a village load profile represented by the two time series contained in the ASCII data files power.txt and pf.txt.

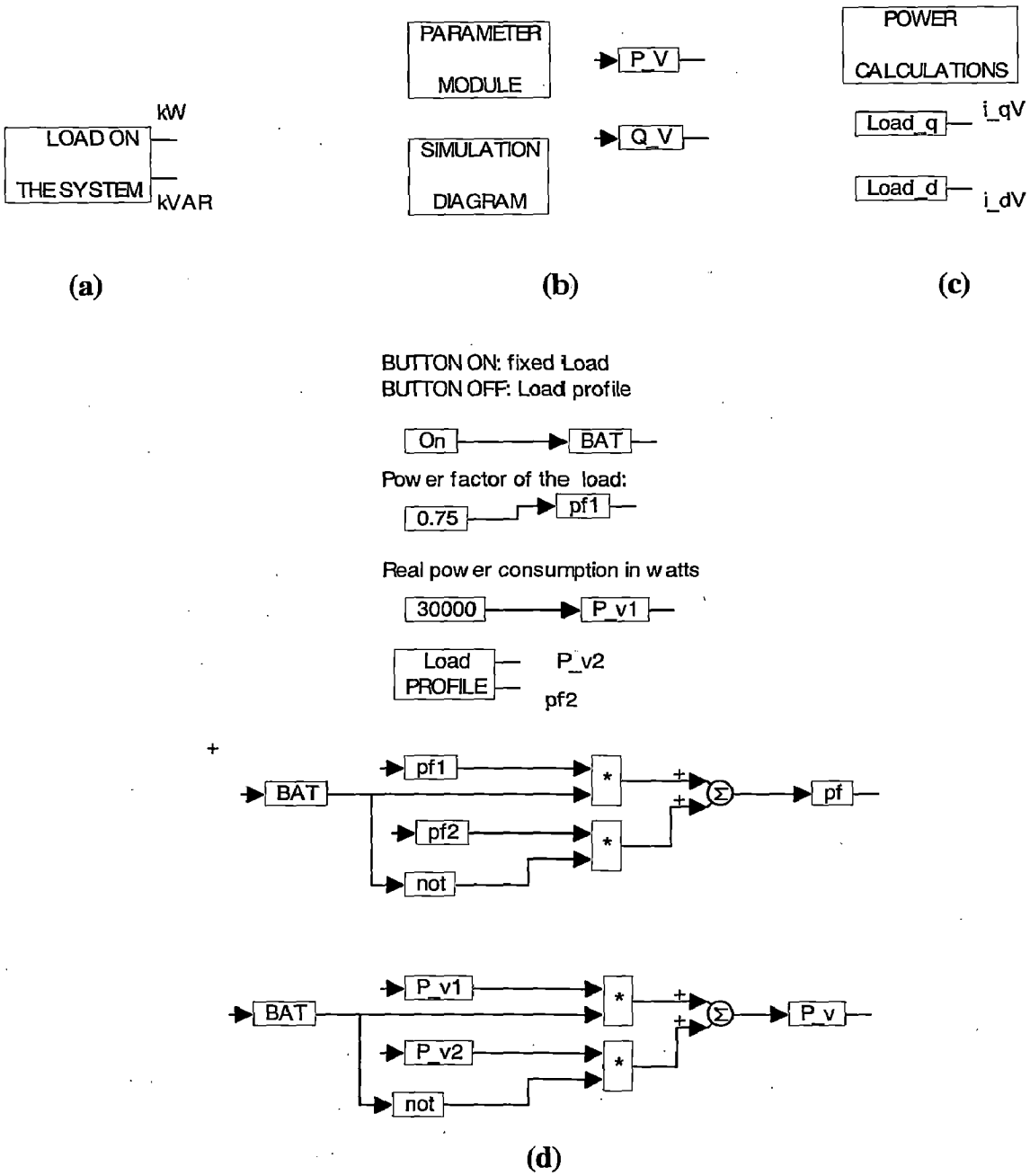

Figure 3.3.9: Block diagrams of the Load module: (a) representation of the Load module in simulation diagrams, (b) first-level expansion, (c) second-level expansion of the simulation diagram, and (d) second-level expansion of the parameter module.

We can modify these data files according to the load profile to be represented or set up our own import block in VisSim. To open these files we must click on Load Profile [Figure 3.3.9(d)] and then on the blocks shown in Figure 3.3.10. The dialog box Import Setup comes up with a button Browse Data. Clicking on this button opens the data files in Notepad. The data files involved must have the format shown in Figure 3.3.10, where the first column is the time and the second column is the value of the variable. In Figure 3.3.11, the compound blocks, which appear in Figure 3.3.9(c), are expanded. Figure 3.3.11(a) shows how both components of the load current are calculated. These calculations are realized by implementation of the equations describing the circuit diagram presented in Figure 3.3.12. First, however, it is necessary to determine the equivalent rated village load parameters: the resistance R_v and the inductance L_v. These, as shown in the upper part of Figure 3.3.11(a), are found by simulation of the following equations (3.46) & (3.47):

$$\frac{P_v}{3} = \frac{V_{s\_ref}^2}{R_v}, \qquad \frac{Q_v}{3} = \frac{V_{s\_ref}^2}{X_v}, \qquad L_v = \frac{X_v}{\omega_b}, \tag{3.46}$$

where the rated reactive power Q_v is defined as

$$Q_v = \sqrt{S_v^2 - P_v^2} = \sqrt{\left(\frac{P_v}{pf}\right)^2 - P_v^2} \tag{3.47}$$

with $S_v = P_v / pf$ being the apparent power. The equations mentioned above, describing the circuit diagram in Figure3.3.12, are implemented here to generate the components of the load current, and are listed below separately for each component. For the q-axis component, the equations given in [(3.48)-(3.50)] read

$$i_{qv} = i_{qV1} + i_{qV2}, \tag{3.48}$$

$$i_{qV1} = \frac{v_{qs1}}{R_v}, \tag{3.49}$$

$$i_{qV2} = \frac{1}{L_v}\int (v_{qs1} - \omega i_{dv} L_v)dt\,. \tag{3.50}$$

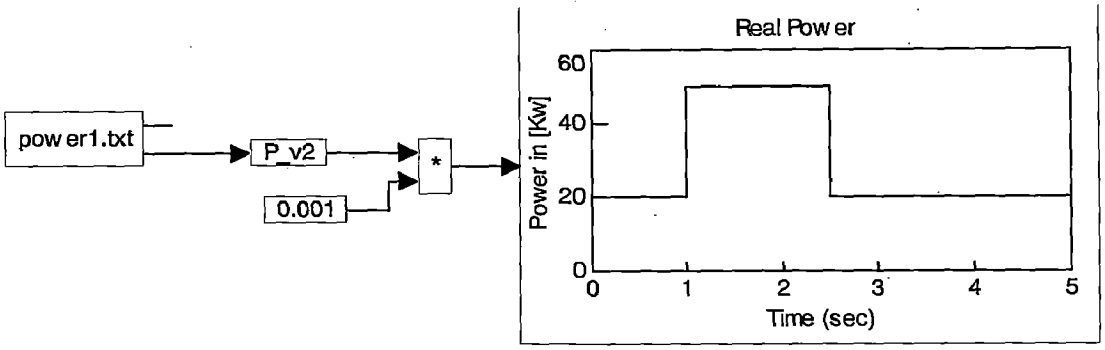

(a)

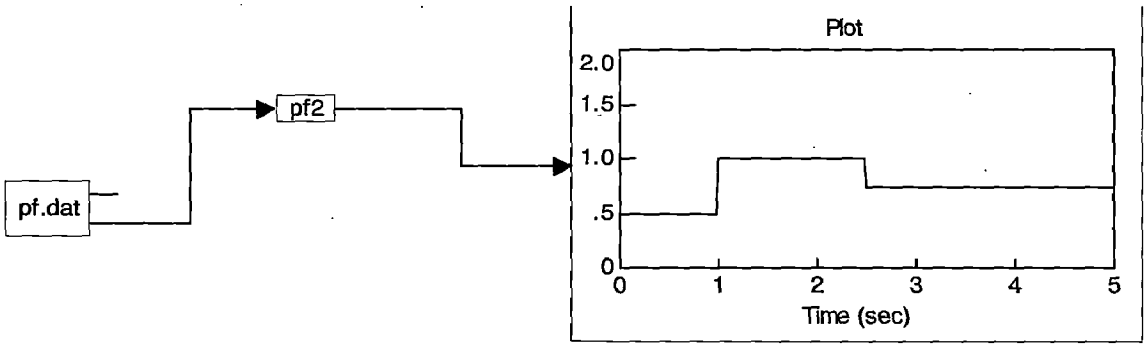

(b)

Figure 3.3.10: An example of a load profile represented graphically. (a)Power in Kw and (b)Power factor.

And the corresponding data values for the Power and Power factor respectively are as below:

Power.txt

0.0000000e+000	2.0000000e+004
0.9999999e+000	2.0000000e+004
1.0000000e+000	5.0000000e+004
2.4999999e+000	5.0000000e+004
2.5000000e+000	2.0000000e+004
2.0000000e+001	2.0000000e+004

Power Factor.txt

Time in (sec)	Power Factor
0.0000000e+000	0.5000000e+000
0.9999999e+000	0.5000000e+000
1.0000000e+000	1.0000000e+000
2.4999999e+000	1.0000000e+000
2.0000000e+001	0.7500000e+000

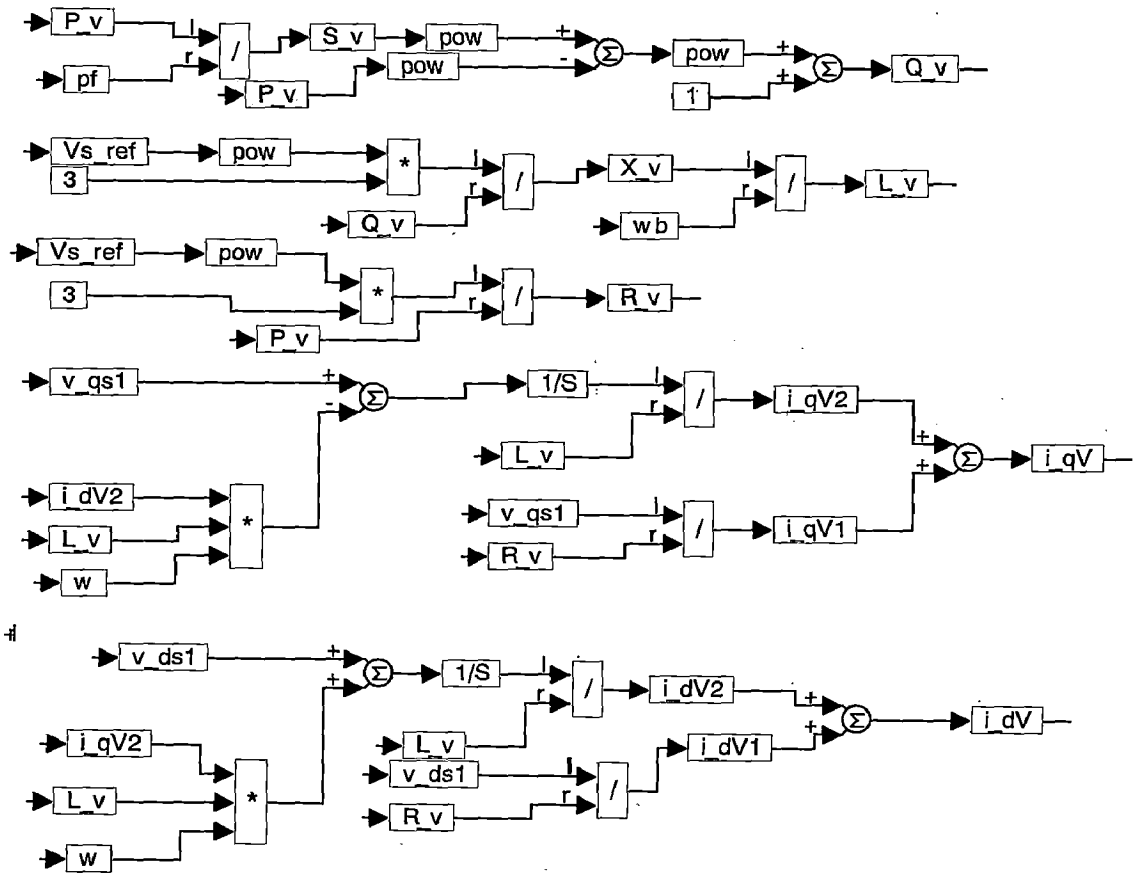

(a)

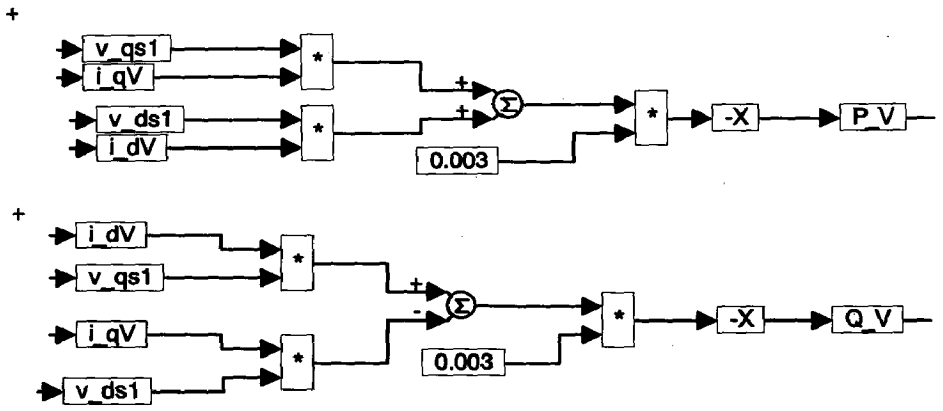

(b)

Figure 3.3.11: Expansions of the compound blocks shown in Figure 3.3.9(c): (a) calculations of the q and d components of the village load currents and (b) power calculations

Similarly, for the d-axis component, the equations [(3.51)-(3.53)] are as follows

$$i_{dv} = i_{dV1} + i_{dV2} \tag{3.51}$$

$$i_{dV1} = \frac{v_{ds1}}{R_v} \tag{3.52}$$

$$i_{dV2} = \frac{1}{L_v}\int (v_{ds1} + \omega i_{qv} L_v)dt \tag{3.53}$$

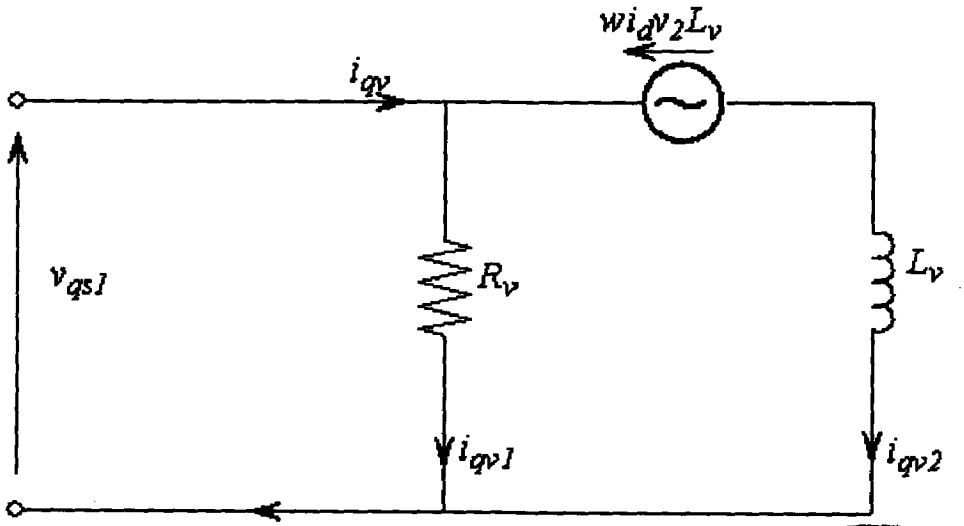

(a)

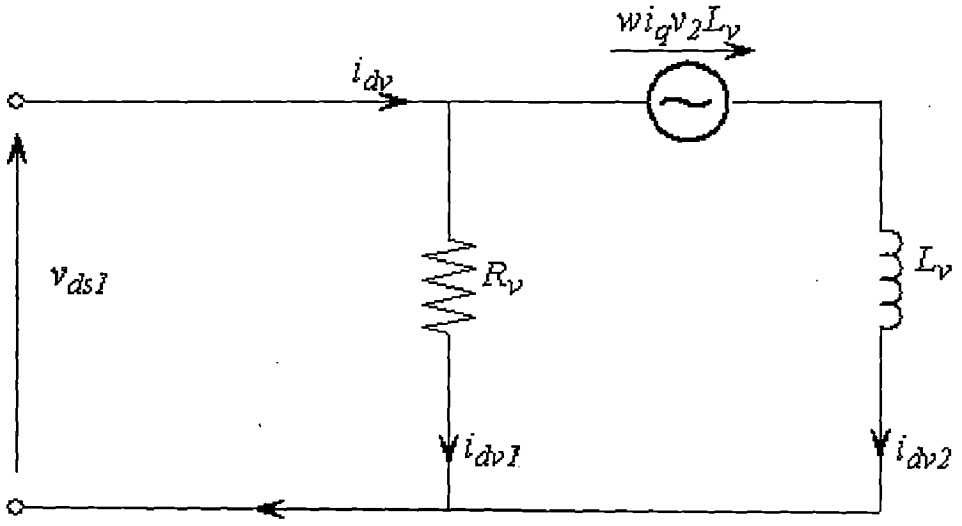

(b)

Figure 3.3.12: Circuit diagram explaining calculationsof the load currents: (a) q-axis and (b) d-axis.

Finally, the calculations of the real power P_V and the reactive power Q_V are implemented in Figure 3.3.4(b), according to the equations (3.54) & (3.55):

$$P_V = -3\times10^{-3}(v_{qs1}i_{qV} + v_{ds1}i_{dV}) \text{ [kW]}, \tag{3.54}$$

$$Q_V = -3\times10^{-3}(v_{qs1}i_{dV} - v_{ds1}i_{qV}) \text{ [kVAR]}. \tag{3.55}$$

P_V and Q_V are computed based on the general convention in this program package, meaning that both P_V and Q_V are negative because village load always absorbs the real power and the reactive power (inductive load).

Chapter 04
SIMULATION RESULTS AND DISCUSSIONS

In this chapter, the performance the hybrid power system modeled is simulated by considering two case studies. In all the case studies that follow, it is assumed the following power sign convention:

- Power generated is positive.
- Power consumed is negative.

Case Study 1: Operation with the Diesel Generator Alone

Principal modules in this case study include:

- A diesel generator with a rated power of 200 kW
- A Load of 50 kW at the power factor pf = 0.75, switched to 150 kW at t = 6 sec, and switched again to 75 kW at t = 12 sec. which is load profile (a) shown in fig.4.2(g).

A power system with this configuration is presented in Figure 4.1, where we show both the single-line diagram and the top-view simulation diagram. This simulation diagram is obtained by adding the following files to the simulation screen: PCC_m.vsm, DG_m.vsm, and VL.vsm. For this system, we obtained traces of power, voltage, and frequency as shown in Figure 4.2. Next, we explain the sequence of simulation events documented in Figure 4.2.

Time/Event Sequence

t = 0	The Diesel generator starts up. This is shown in Fig (a)
t = 4 sec	Line voltage V_s reaches the reference value of 266 V; the relative frequency is close to 1.
	Power generated by the diesel generator is at the level of 50 kW; the same power is consumed by the Load. It can be observed from fig (a) and (b)
t = 6 sec	The Load is increased to 150 kW.

This increment is followed by the sharp increase to the value of 150 kW of the power that the diesel generator provides to the system. Transient small dips of frequency and line voltage can be seen.

t = 12 sec — The Load is reduced to 75 kW.

Power generated by the diesel generator decreases sharply to this value.

Transient small jumps of frequency and line voltage can be seen. The above two observations are shown in the below figures.

t >16 sec — Steady state is reached with all variables constant.

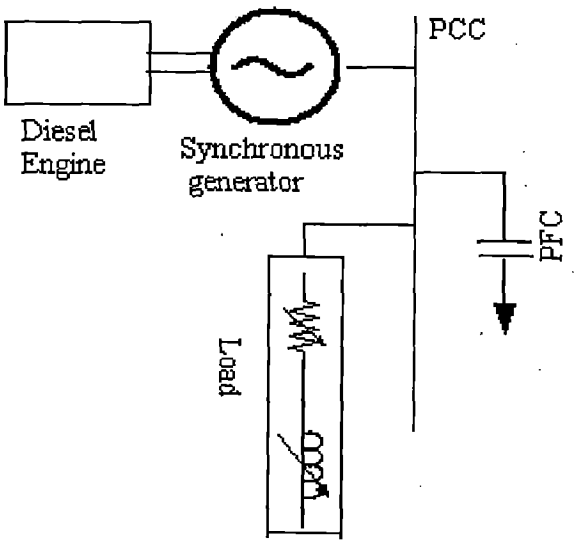

(a)

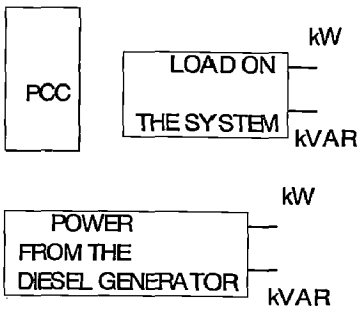

(b)

Figure 4.1: Power system composed of a DG and a Load: (a) single-line diagram and (b) Top view of the VIS-SIM simulation.

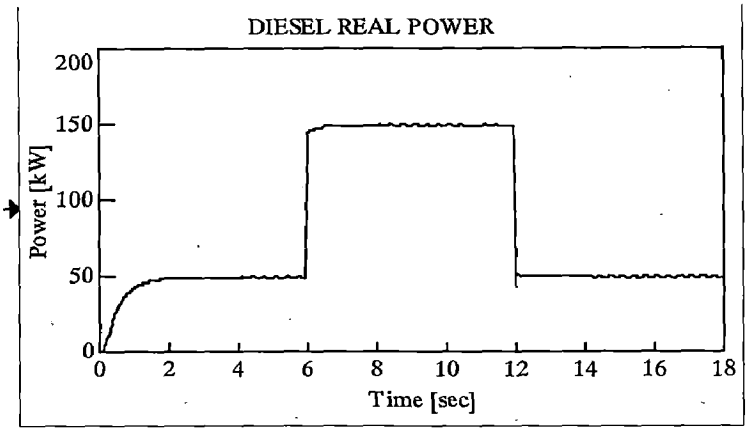

(a) Diesel Real Power

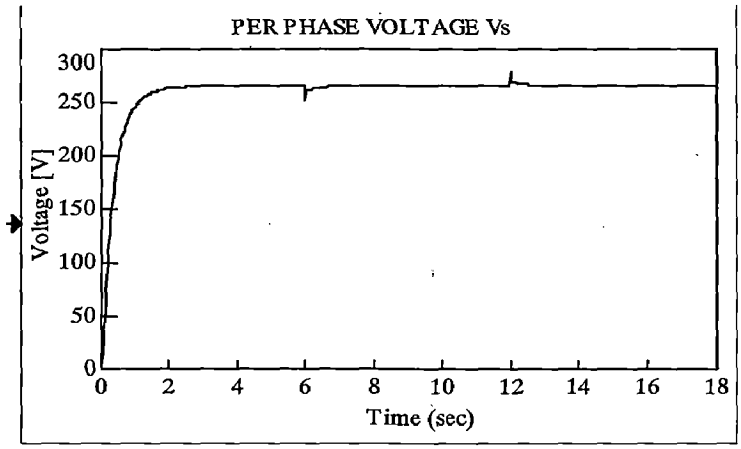

(b) Voltage (RMS)

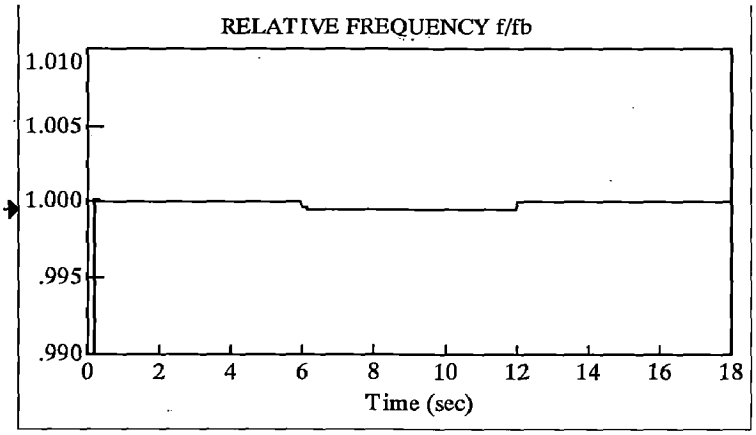

(c) Supply frequency

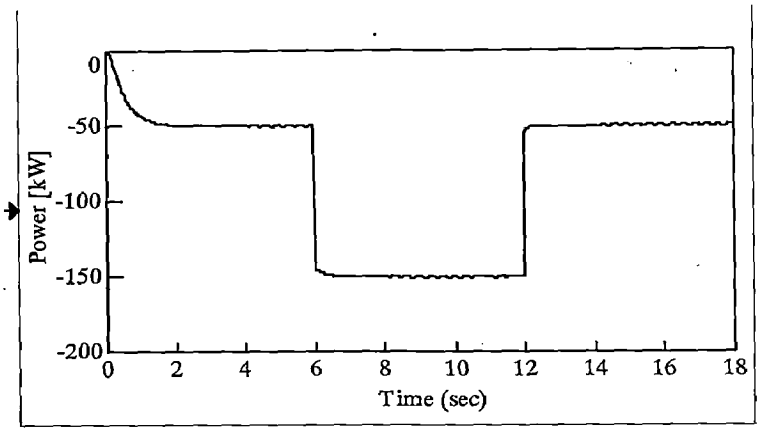

(d) Active Load on the System in Kw

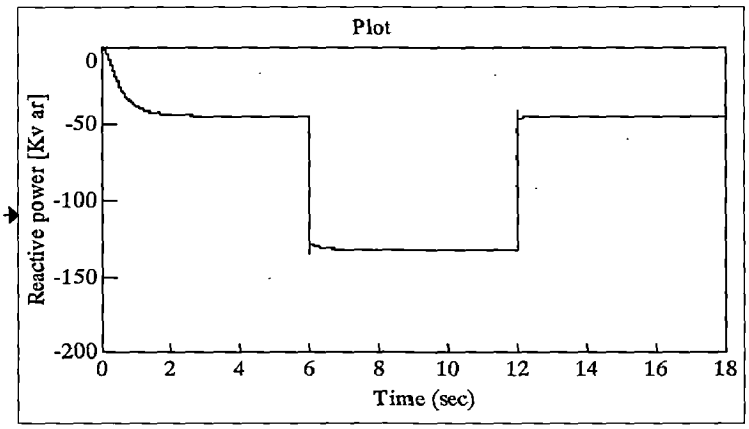

(e) Reactive Load on the System in Kvar

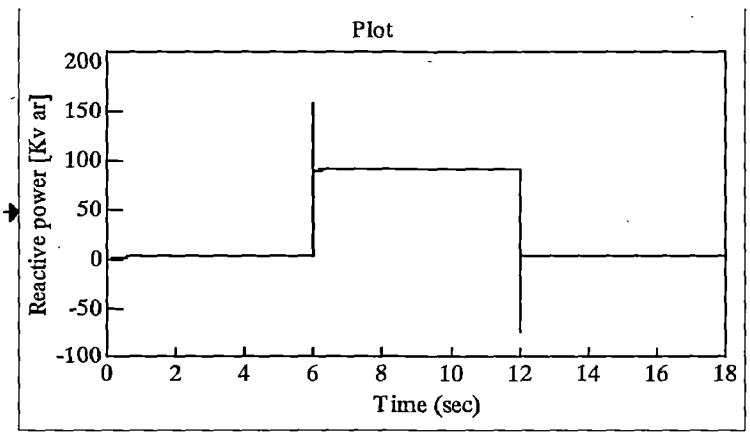

(f) Reactive Power from the Diesel generator

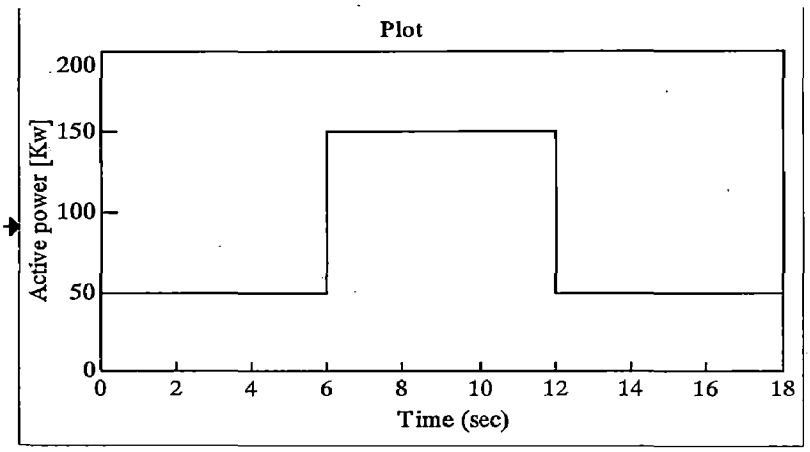

(g) Load profile (Active) in Kw

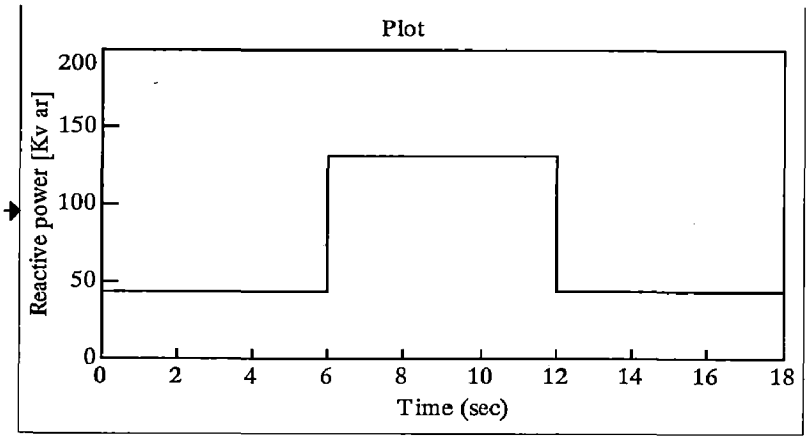

(h) Reactive Load Profile in Kvar

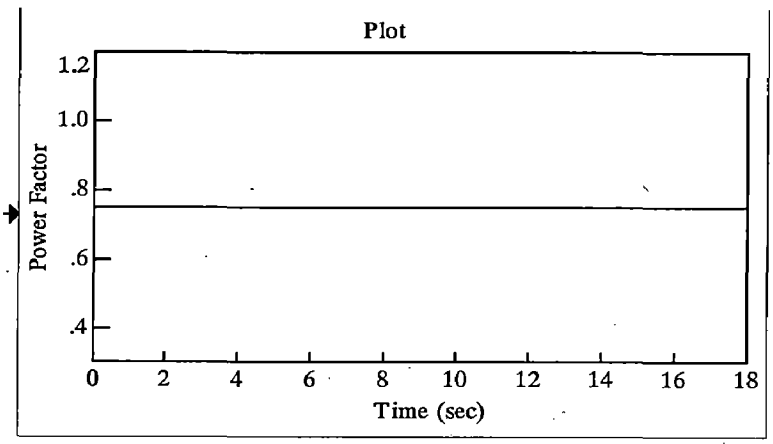

(i) Power Factor of the Load

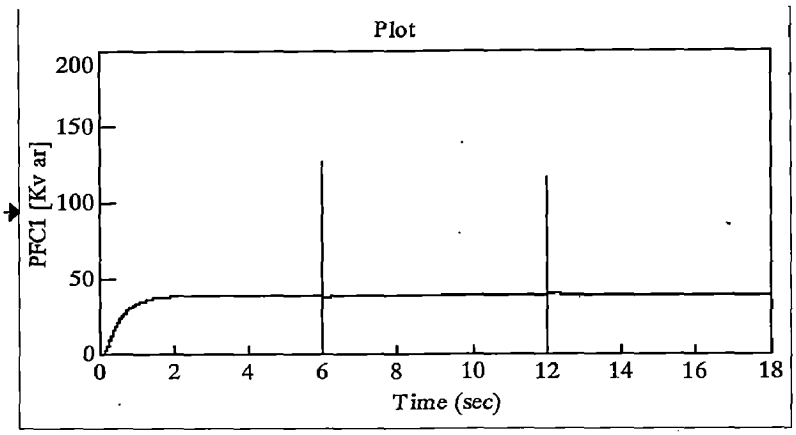

(j) Reactive power supplied from the Capacitor

Figure 4.2: Traces of power, voltage, and frequency for the system composed of a DG and a variable Load at a constant power factor

Case 1-b

- For the same system as in case 1, but the different load profile i.e., load profile (b) which is shown in fig.4.3(f), with variable power factor the results are as follows:

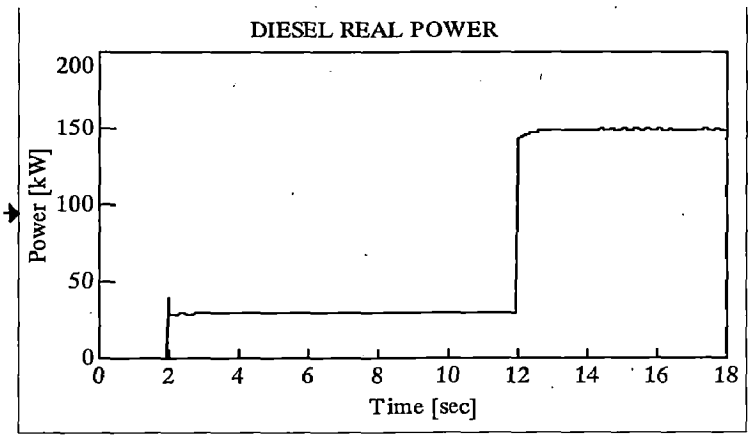

(a) Diesel Real Power

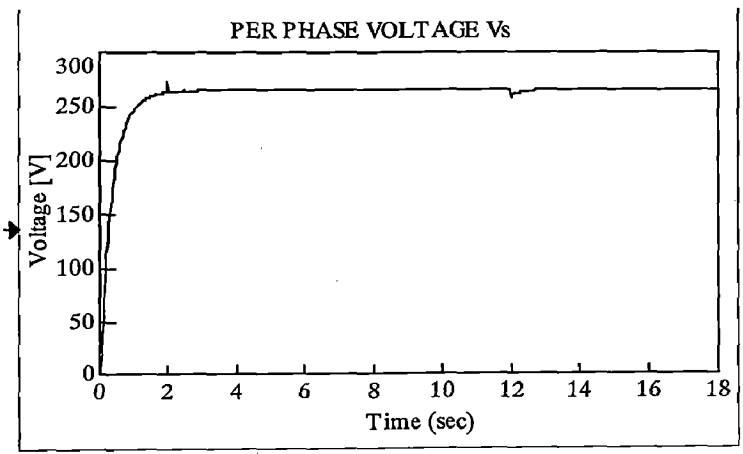

(b) Voltage (RMS)

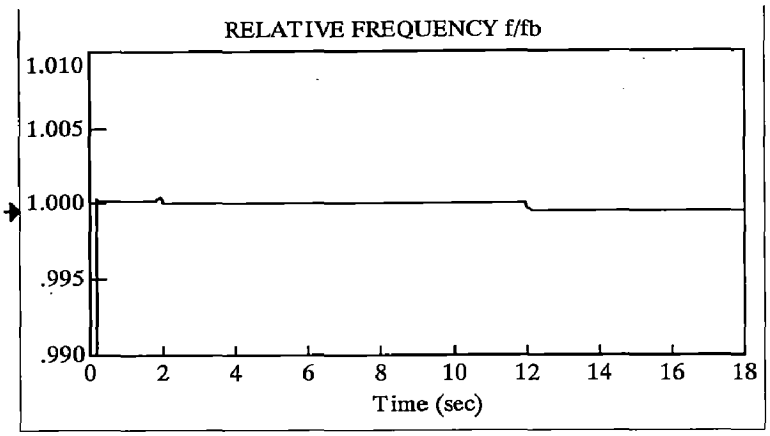

(b) Supply frequency

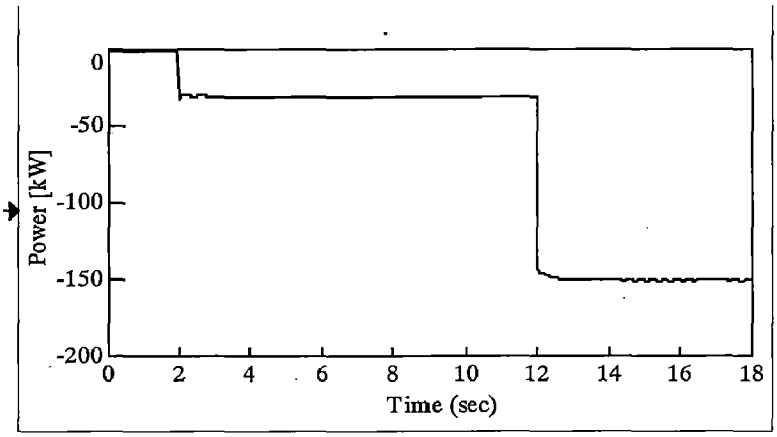

(d) Active Load on the System in Kw

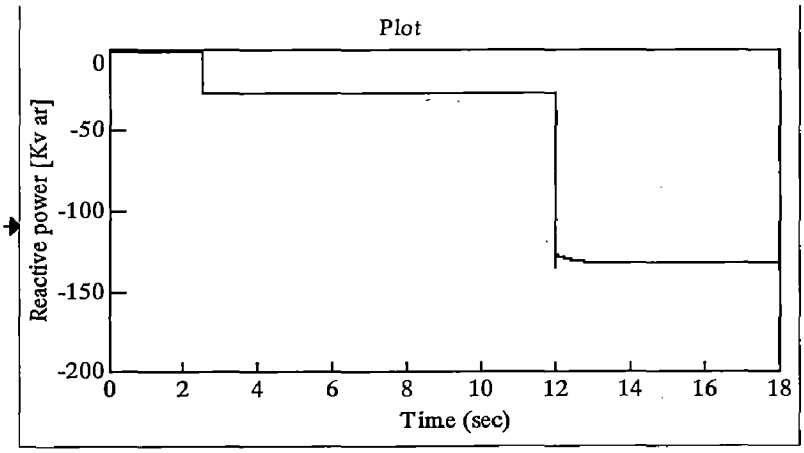

(e) Reactive Load on the System in Kvar

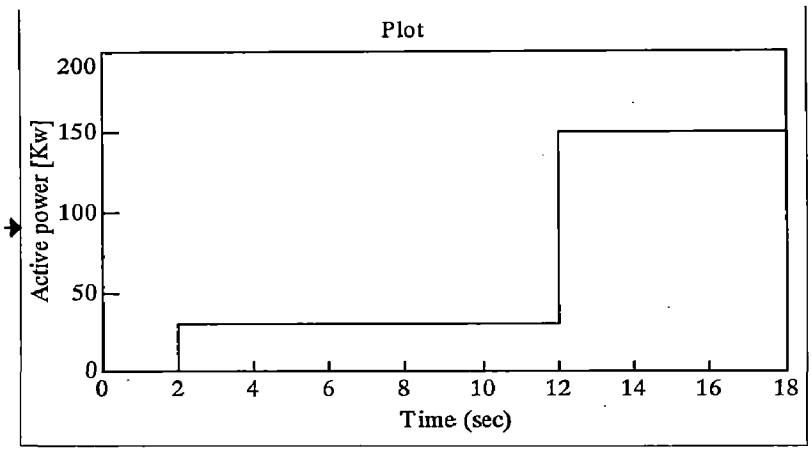

(f) Active Load Profile

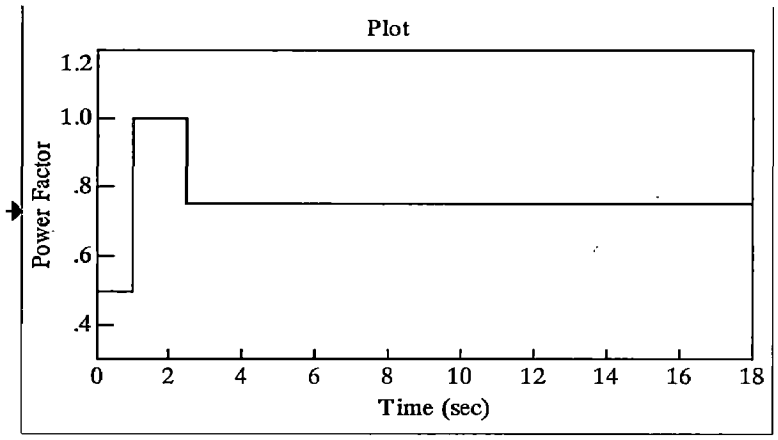

(g) Load Power Factor

Figure 4.3: Traces of power, voltage, and frequency for the system composed of a DG with a variable Load and power factor

Case Study 2: operation of the system with wind farm and diesel

Principal modules in this case study include:

- A diesel generator with a rated power of 200 kW
- An AC WT driven by the wind, given by a file of the wind speed time series
- A load of 30 kW at the power factor pf = 0.75.

A power system with this configuration is presented in Figure 4.3, where we presented both the single-line diagram and the top-view VIS-SIM simulation diagram. The simulation diagram is obtained by adding the following files to the simulation

screen: PCC_m.vsm, DG_m.vsm, VL.vsm, and wtg_base_m.vsm. For this system, we obtained traces of power, voltage, and frequency as shown in Figure 4.4. Next, we explain the sequence of simulation events documented in Figure 4.4.

Time/Event Sequence

t = 0	The Diesel generator starts up.
t = 2.5 sec	Line voltage V_s reaches the reference value of 266 V; the relative frequency is 1. Power generated by the diesel generator is at the value of 30 kW the same power is consumed by the load.
t = 6 sec	The induction machine starts to motor the wind turbine and creates a large load. Power generated by the diesel generator increases sharply. Transient small frequency and line voltage dips are observed.
t = 7 sec	Power consumption of the induction machine, reaching the synchronism, rapidly drops.
t = 7.25 sec	The Wind turbine generator starts to generate. Power generated by the diesel generator decreases below 30 kW, which is the consumption level of the Load.
t > 12.5 sec	Power generated by the wind turbine generator increases because of a wind gust.

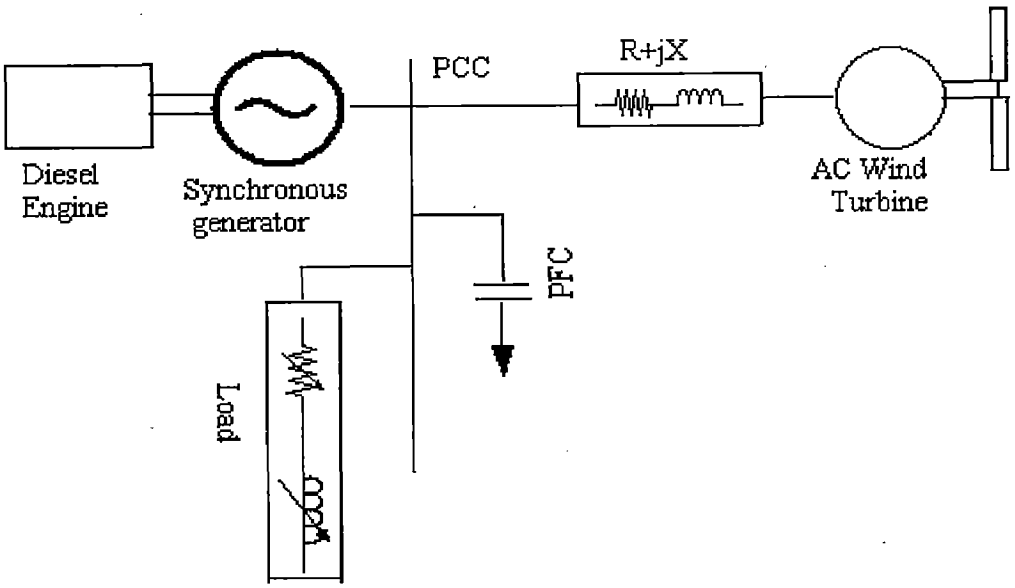

(a)

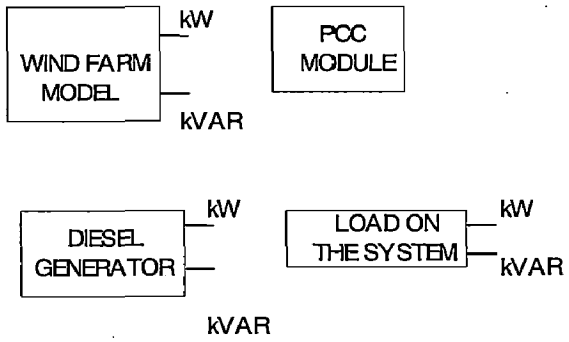

(b)

Figure 4.4: Power system composed of a DG, an AC WT, and a Load: (a) single-line diagram and (b) top view of the VIS-SIM simulation

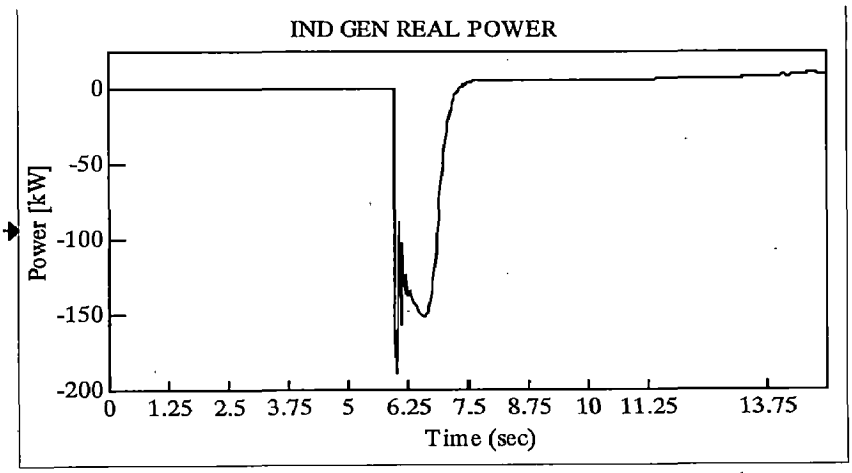

(a) Power supplied by the wind farm

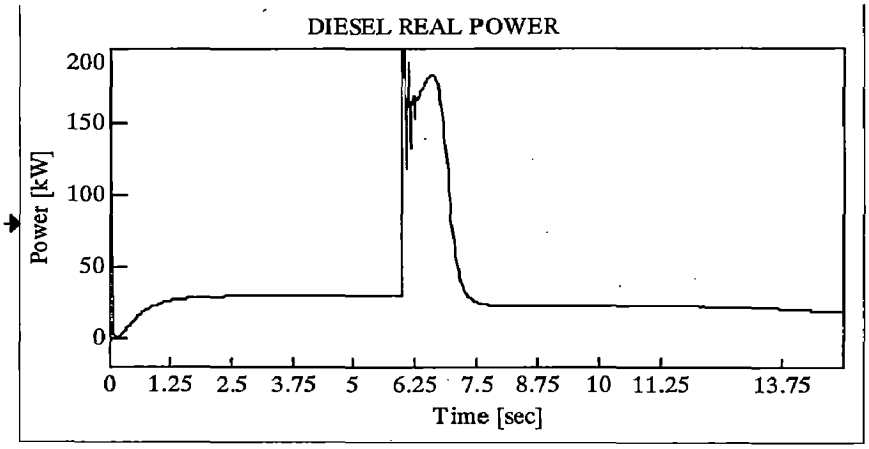

(b) Power supplied by the DG

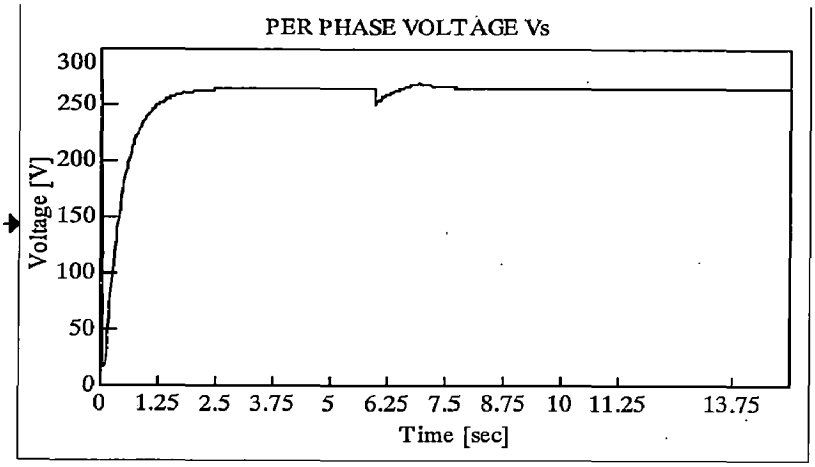

(c) Supply voltage

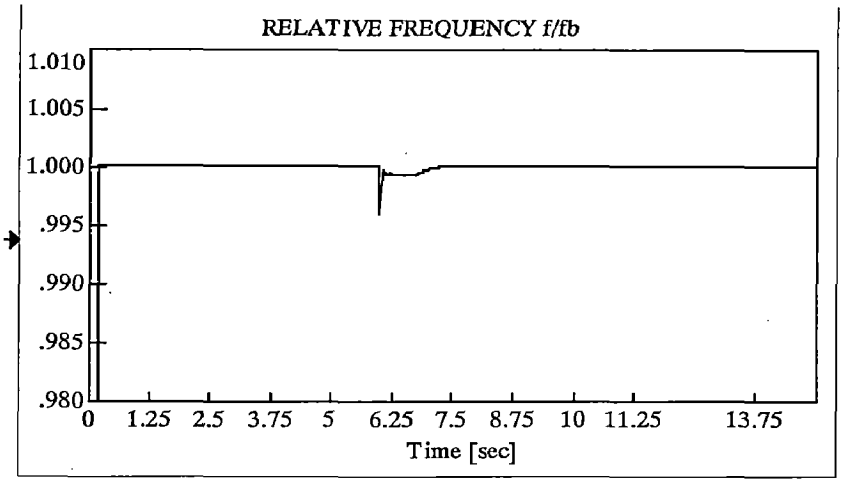

(d) Supply frequency

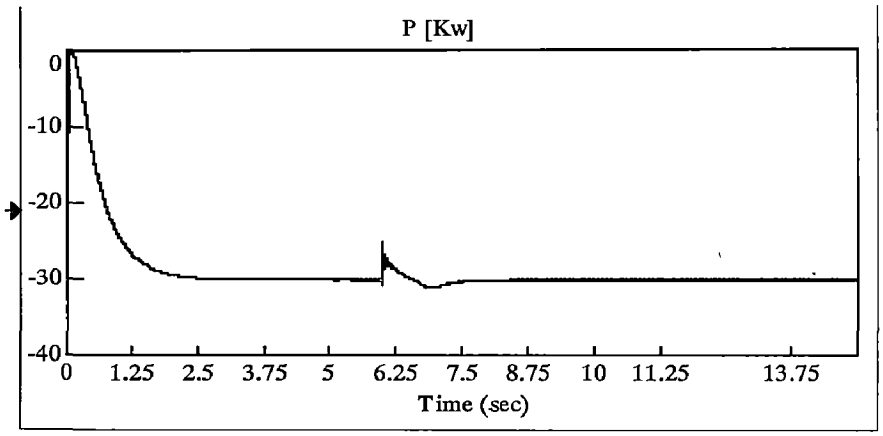

(e) Load on the system in Kw

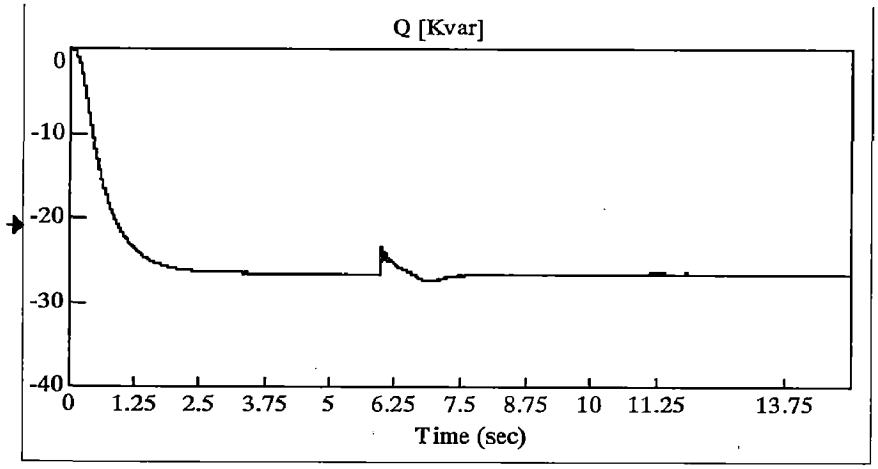

(f) Reactive load on the system in Kvar

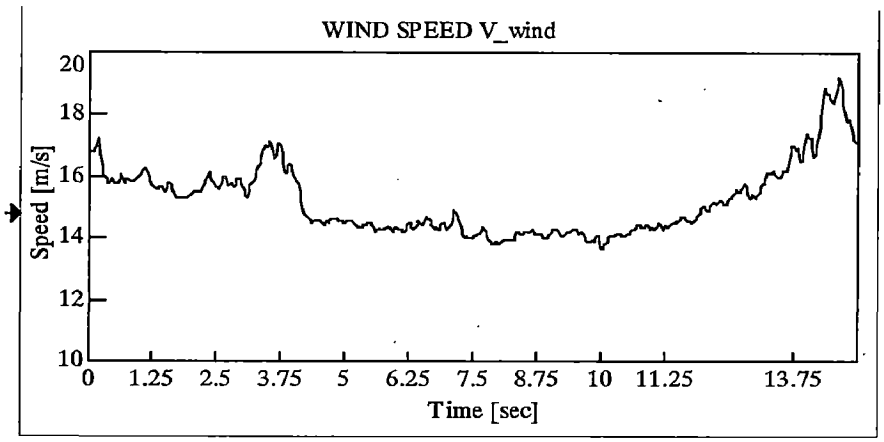

(g) Variable wind speed

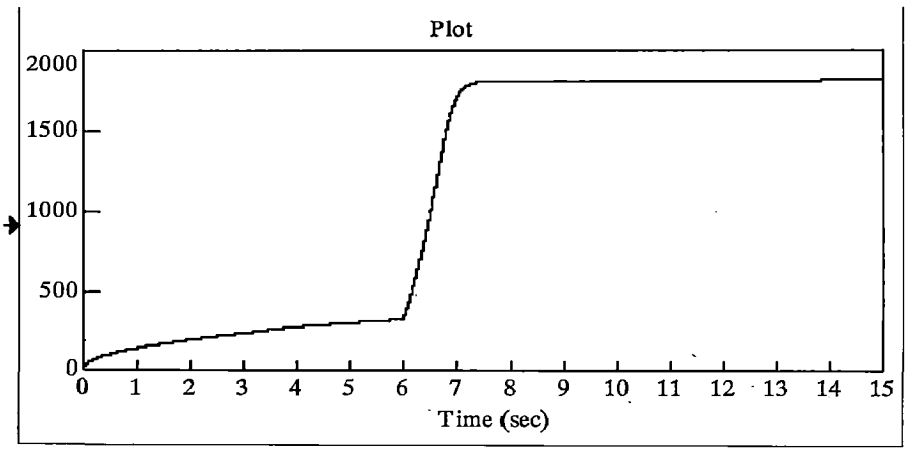

(h) Speed of Induction machine in rpm

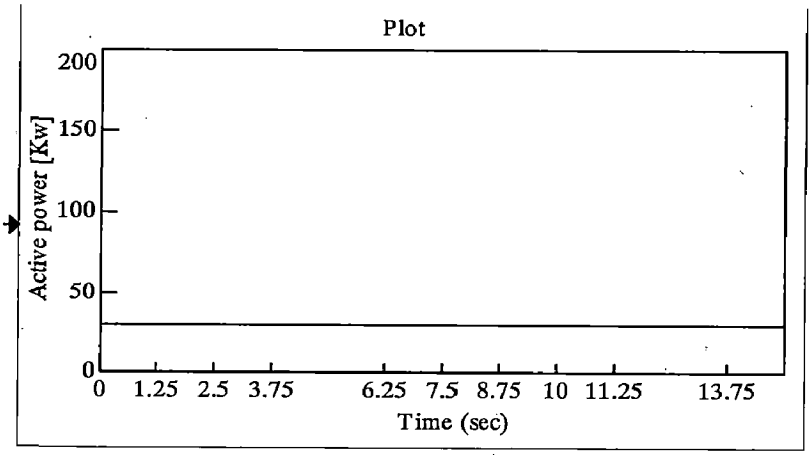

(i) Load profile in Kw

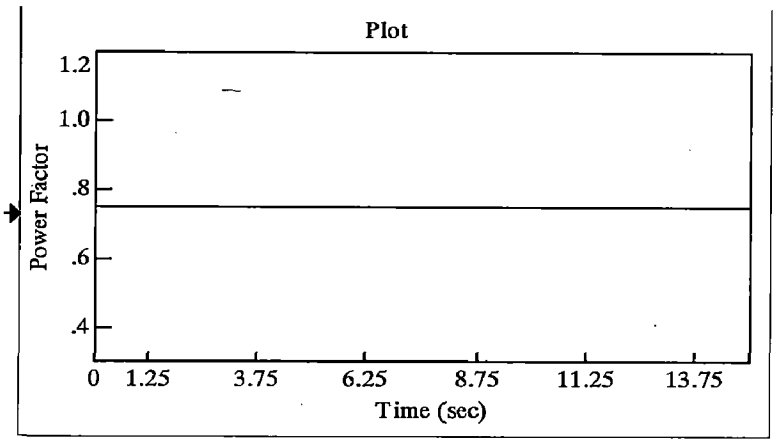

(j) Load power factor

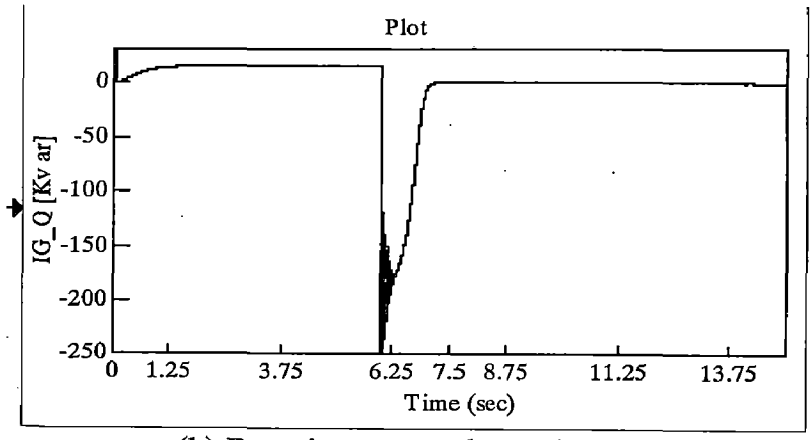

(k) Reactive power drawn by IM

Figure 4.5: Traces of power, voltage, and frequency for the system composed of a DG, an AC WT, and the constant Load

Chapter 05
CONCLUSION AND SCOPE FOR FUTURE WORK

A Computer simulation based model of a hybrid generation system comprising of a wind energy conversion system and a diesel generation system is presented. This work starts with an overview of the components of the power system under investigation. The developed model is used to evaluate the performance of the hybrid generation system (diesel-wind turbine) with varying wind speeds and different load conditions. Simulation results indicate that the developed model has the ability to meet both real and reactive power requirements of the load, maintaining prescribed values of voltage and frequency, with the help of the voltage and speed regulators. In all the case studies the diesel generator controls the system's voltage and frequency. The modelling of the various power system components was examined. Models were given for the various components of an autonomous power system that is for conventional units (Diesel engine, synchronous generator and speed and voltage regulators), for wind generators (wind turbine, asynchronous generator), for capacitor banks, for the transmission network and finally for various types of loads. The integration of the models presented here in simulation software will provide a general and robust tool for the accurate assessment of isolated Diesel-wind turbine system interaction. The wind turbine contributed significantly to the load, thus reducing the fuel consumption of the diesel generator when the wind speed was available. From the simulation results we have observed the reasons for the frequency and voltage fluctuation.

The following factors contribute to frequency fluctuation:

- Large real power surges during start-up of the induction motor, wind power fluctuations, etc.
- Slow response of the governor control at the diesel side.
- Frequency dip when the diesel engine is loaded by a sudden large load or the diesel engine is under-rated with respect to the load.
- Frequency run-away when the wind turbine produces more power than needed. In this case, the diesel engine looses control of its rotor speed.

- Change in generator set frequency that may affect the operation of the induction generator (i.e., during frequency fluctuation, the induction generator may enter the motoring region for a very short period of time).

The following factors contribute to voltage fluctuation:

- Voltage drop across the line impedance caused by large current surges.

Current surges can be developed at the start-up of an induction machine operating from fixed frequency (large induction machines). In particular, they produce reactive current surges.

Reduction to current surges can be accomplished as follows:

- ✓ For wind turbines with a dual-winding generator, use smaller-sized induction machines during start-up, connect the generator when the rpm starts rotating close to the synchronous speed of the generator. Or, use a soft start to control the stator current.
- ✓ For other large loads (water pumps or compressors), use a soft-start device to limit the current surges, use variable frequency drives if affordable, use sequential start-up when appropriate.
- Slow response of the exciter as the synchronous generator side reactive power mismatch.
- Uncoordinated capacitor switching.

In this thesis a variable speed wind energy conversion system has been presented. The response of the simulated model was observed with dynamic load and changing wind conditions. Modeling and analysis of the induction generator, the electrical generator used in this thesis, was explained in detail using dq-axis theory. For modelling of all components of power systems the simulation software has been used as VisSim 6.0. From the simulation results presented, it can be said that the induction generator is inherently capable of operating at variable speeds. The induction generator can be made to handle almost any type of load. Induction generator as the electrical generator is an ideal choice for isolated variable-wind power generation schemes, as it has several advantages over conventional synchronous machine.

Scope for Future Work

- Different DG systems (i.e. microturbine generation, fuel cells, photovoltaic etc.) can be used for hybrid power systems to study their interaction instead of diesel and wind which is used in this work.
- Other type of DG interaction related to power quality like voltage unbalance, harmonics can also be studied.
- Different mitigating the adverse effects of DG in the hybrid power system using the fact devices like STATCOM can also be considered.
- Artificial intelligence techniques can be devised effectively to control the adverse effects of DG system on the power system.
- Intelligent controls could be very helpful in designing of speed and voltage regulators for maintains the required voltage and frequency.
- Modelling of other components such as storage system (i.e. battery) can be included in the system to store the excess power which comes when ever the total hybrid generation (sum of wind generation and diesel generation) exceeds the load on the system.
- The developed system can be operated with the high wind penetration if we include the dump load and its control switch in to the system.
- The system performance can be studied with the different faults, which may be on induction machine, synchronous machine or on the power system.

[01] G. Pepermans, J. Driesen, D.Haeseldonckx, R.Belmans, W.D.haeseleer, *"Distributed Generation: Definition, Benefits and Issues,"* Energy Policy 33 (2005) Pages.787–798

[02] Ramnarayan Patel, Satish Kumar Singh, S. Panda, *"Distributed Generation as A Power Paradigm for the New Millennium,"* IEE PESTICON Jan 29-30,2005, Kolkatta, India

[03] P. P. Barker and R.W. de Mello, *"Determining the Impact of Distributed Generation on Power Systems: Part 1—Radial Distribution Systems,"* in Proc. IEEE Power Eng. Soc. Summer Meeting, vol. 3, 2000, pp.1645–1656.

[04] N Jenkins and G Strbac, *"Effects of Small Embedded Generation on Power Quality," IEE Colloquium on "Issues in Power Quality,"* Warwick-28th November 1995.

[05] Visual simulation software available http://www.vissim.com/downloads/vswork_d.html

[06] Visual simulation manual available ftp://ftp.vissim.com/pub/Documentation/Version_6/SisSim_UGv60.pdf

[07] C.P.Butterfield, Eduard Muljadi, *"Pitch Controlled Variable-Speed Wind Turbine Generation,"* IEEE transactions on industry applications, Vol.37, No.1, January/February 2001

[08] Eduard Muljadi, H.E. McKenna, *" Power Quality Issues In Hybrid Power System,"* Industry Applications Conference, 2001 Volume 2, 30 Sept.-4 Oct. 2001

[09] J.G.Slootweg, S.W.H.de Haan, H.Polinder, W.L.Kling, *"General Model for Representing Variable Speed Wind Turbines In Power System Dynamic Simulations,"* IEEE Transactions On Power Systems, Vol.18, No.1, February 2003

[10] Tomas Petru, Torbjorn Thiringer, *"Modeling of Wind Turbines for Power System Studies,"* IEEE Transactions On Power Systems, Vol.17, No.4, November 2002

[11] N. A. Schinas, N. A. Vovos, G. B. Giannakopoulos, *"An Autonomous System Supplied Only By A Pitch Controlled Variable Speed Wind Turbine,"* IEEE transactions on energy conversion, June13 2005

[12] Kim Johnsen, Bo Eliasson, *"Simulink Implementation of Wind Farm Model For Use In Power System Studies,"* Nordic wind power conference, 1-2 March, 2004, Chalmers university of technology

[13] Antonios E.haniotis, Konstantinos S.Soutis, Antonios G.Kladas, John A.Tegopoulos, *"Grid Connected Variable Speed Wind Turbine Modeling, Dynamic Performance and Control,"* IEEE transactions on power systems, 2004

[14] P.C.Krause, C.H.Thomas, *"Simulation of Symmetrical Induction Machinery,"* IEEE Transactions on Power Apparatus And Systems, Vol.84, pp.1038-1053, November 1965.

[15] Anca D.Hansen, Florin Iov, Poul Sorenson, Frede Blaabjerg, *"Overall Control Strategy of Variable Speed Doubly-Fed Induction Generator Wind Turbine,"* Nordic Wind Power Conference, 1-2 March, 2004, Chalmers University of technology, Sweden

[16] R.C. Bansal, T.S. Bhatti, D.P. Kothari, *"Bibliography on the Application of Induction Generators in Non conventional Energy Systems"* Energy Conversion, IEEE Transactions on Volume 18, Issue 3, Sept. 2003 Page(s):433 – 439.

[17] Kundur P., *"Power System Stability and Control"*, McGraw Hill Inc., New York

[18] Padiyar K.R., *"Power System Dynamics- Control and Stability"*, Interline Publishing Pvt. Ltd., Bangalore.

[19] Anderson P.M. and Fouad A.A., *"Power System Control and Stability,"* Vol. 1, 1st edition, The lowa state university press, Ames, lowa, USA.

[20] Eduard Muljadi, H.E. McKenna, " *Power Quality Issues In Hybrid Power System,"* IEEE Trans. Industry Applications, Vol. 38, No. 3, May/June 2002

[21] J.T. Bialasiewicz, E. Muljadi, S. Drouilhet, G. Nix, *"Hybrid Power Systems with Diesel And Wind Turbine Generation,"* American Control Conference, 1998. Volume 3, 24-26 June 1998 Page(s):1705 – 1709

[22] MATLAB/Simulink SimPowerSystems Documentation. Available: http://www.mathworks.com

[23] C.Wang, E.Muljadi, M.H.Nehrir, *"Parallel Operation of Wind Turbine, Fuel Cell, And Diesel Generation Sources,"* IEEE Power engineering society, June 6-June 10, 2004

[24] A.Tomilson, J.Quaicoe, R.Gosine, M.Hinchey, N.Bose, *"Modeling An Autonomous Wind-Diesel System Using Simulink,"* IEEE transactions on power systems, 1997

[25] G.S.Stavrakakis, G.N.Kariniotakis, *"General Simulation Algorithm for The Accurate Assessment of Isolated Diesel-Wind Turbines Systems Interaction,"* IEEE transactions on energy conversion, Vol.10, No.3, September 1995.